Robust Wireless Relay Networks: Slow Power Allocation With Guaranteed QoS

Tony Q. S. Quek, *Student Member, IEEE*, Hyundong Shin, *Member, IEEE*, and Moe Z. Win, *Fellow, IEEE*

***Abstract*—In wireless networks, power allocation is an effective technique for prolonging network lifetime, achieving better quality-of-service (QoS), and reducing network interference. However, these benefits depend on knowledge of the channel state information (CSI), which is hardly perfect. Therefore, robust algorithms that take into account such CSI uncertainties play an important role in the design of practical systems. In this paper, we develop relay power allocation algorithms for noncoherent and coherent amplify-and-forward (AF) relay networks. The goal is to minimize the total relay transmission power under individual relay power constraints, while satisfying a QoS requirement. To make our algorithms practical and attractive, our power update rate is designed to follow large-scale fading, i.e., in the order of seconds. We show that, in the presence of perfect global CSI, our power optimization problems for noncoherent and coherent AF relay networks can be formulated as a linear program and a second-order cone program (SOCP), respectively. We then introduce robust optimization methodology that accounts for uncertainties in the global CSI. In the presence of ellipsoidal uncertainty sets, the robust counterparts of our optimization problems for noncoherent and coherent AF relay networks are shown to be an SOCP and a semi-definite program, respectively. Our results reveal that ignoring uncertainties associated with global CSI often leads to poor performance. We verify that our proposed algorithms can provide significant power savings over a naive scheme that employs maximum transmission power at each relay node. This work highlights the importance of robust algorithms with practical power update rates in realistic wireless networks.**

***Index Terms*—Amplify-and-forward, linear program, quality-of-service, relay networks, robust optimization, semi-definite program, slow power allocation.**

I. Introduction

RESOURCE allocation in wireless networks promises significant benefits such as longer network lifetime, better quality-of-service (QoS), and lower network interference. In relay networks, the primary resource is the transmission power because it affects both the lifetime and the scalability of the network. For example, consider a wireless sensor network where sensor nodes have limited power resources, such as a battery or solar based source. To prolong network lifetime, it is important to determine the optimal transmission power of the sensor nodes [1], [2]. Furthermore, regulatory agencies may limit the total transmission power to reduce network interference. For example, consider a relay-enhanced cellular network, where nodes are deployed to relay transmissions from a base station to a distant user. In such a network, efficient power allocation can be used to minimize network interference while satisfying certain QoS requirements [3].

In relay networks, various relaying schemes have been proposed and studied [4], [5]. Among these, considerable attention has been placed on decode-and-forward (DF) and amplify-and-forward (AF) relaying. In DF relaying, the relay node fully decodes, re-encodes, and retransmits the source messages. In AF relaying, the relay node simply forwards a scaled version of its received signal. To reduce the required cooperation overhead, these relaying schemes can also be implemented with only a subset of active relay nodes, which are appropriately selected [6]–[9]. Furthermore, many of the recent works have focused on relay power allocation. For DF relay networks, [8], [10]–[13] consider orthogonal relay transmissions while [9], [14] exploit the possibility of performing distributed beamforming over a common bandwidth. The problem formulations include maximizing capacity [11], [14], minimizing outage probability [8], [9], and minimizing transmission power [10], [12]. Similarly, for AF relay networks, [10], [13], [15], [16] consider orthogonal relay transmissions while [17] considers relay transmissions over a common bandwidth. The problem formulations include maximizing capacity [13], [17], minimizing outage probability [16], and minimizing transmission power [10], [15]. In all the above works, power allocation is performed without imposing any individual relay power constraint.

Here, we focus on an AF relay network due to the simplicity of AF relaying, which lends itself to practical implementation. In particular, we consider noncoherent and coherent AF relaying depending on the type of channel state information (CSI) available at each relay node. We consider that all relay nodes operate in a common frequency band. This allows faster and easier deployment of the relay nodes in the network since the addition of relay nodes to the existing network will have little effect on the source and destination nodes, e.g., specific relay channel assignments are not necessary. The goal is to propose a centralized optimization framework for the minimization of total relay transmission power. In a centralized design, the relay nodes need to send their local CSI to the central unit, which determines the

Manuscript received January 31, 2007; revised September 3, 2007. This work was supported in part by the Charles Stark Draper Laboratory Robust Distributed Sensor Networks Program, the Office of Naval Research Young Investigator Award N00014-03-1-0489, the National Science Foundation under Grants ANI-0335256 and ECS-0636519, by DoCoMo USA Labs, and by the Korea Research Foundation Grant funded by the Korean Government (MOEHRD) (KRF-2006-331-D00336). The first author was supported in part by the ASTAR National Science Scholarship. The associate editor coordinating the review of this manuscript and approving it for publication was Dr. Timothy Davidson.

T. Q. S. Quek and M. Z. Win are with the Laboratory for Information & Decision Systems (LIDS), Massachusetts Institute of Technology, Cambridge, MA 02139 USA (e-mail: qsquek@mit.edu; moewin@mit.edu).

H. Shin is with the School of Electronics and Information, Kyung Hee University, Gyeonggi-do, 446-701 Korea (e-mail: hshin@khu.ac.kr).

Color versions of one or more of the figures in this paper are available online at http://ieeexplore.ieee.org.

Digital Object Identifier 10.1109/JSTSP.2007.910271

transmission power of the relay nodes.[1] However, all previous works assume that perfect global CSI is available at the central unit [8]–[17]. In practice, such an assumption is too optimistic since the global CSI is often subject to uncertainties. Moreover, the power allocation algorithms proposed in the above works require the central unit to track the global CSI at the timescale of fast-fading. This requires frequent communication between the relay nodes and the central unit to determine new power allocations. This motivates the design of a robust optimization framework that accounts for CSI uncertainties with practical algorithms that track only the large-scale fading.[2]

In this paper, we formulate the relay power allocation problem as the total relay transmission power minimization problem subject to a QoS constraint.[3] Our algorithms only track the large-scale fading and thereby lead to practical implementations.[4] We show that our optimization problems for noncoherent and coherent AF relay networks can be cast as a linear program (LP) and a second-order cone program (SOCP), respectively, under perfect knowledge of large-scale fading. We introduce robust optimization methodology to account for uncertainties in the global CSI. For ellipsoidal uncertainty sets, the robust counterparts of the power minimization problems for noncoherent and coherent AF relay channels can be formulated as an SOCP and a semi-definite program (SDP), respectively. Numerical results show that our proposed algorithms can provide significant power savings over a naive scheme that employs maximum transmission power at each relay node.

The paper is organized as follows. In Section II, we describe our system model and problem formulation. In Section III, we present the optimal relay power allocation algorithms for the noncoherent and coherent AF relay networks. Next, in Section IV, we formulate the robust counterparts of the power allocation problems. In Section V, we present some numerical results. We give our conclusions in the last section.

Notation: Throughout the paper, we shall use the following notation. Boldface upper-case letters denote matrices, boldface lower-case letters denote column vectors, and plain lower-case letters denote scalars. The superscripts $(\cdot)^T$, $(\cdot)^*$, and $(\cdot)^\dagger$ denote the transpose, complex conjugate, and transpose conjugate, respectively. We denote a vector with all 1 elements as $\mathbf{1}$, a vector with all 0 elements as $\mathbf{0}$, $n \times n$ identity matrix as $\boldsymbol{I}_n$, and (i,j)th element of $\boldsymbol{B}$ as $[\boldsymbol{B}]_{ij}$. The notations $|\cdot|$ and $||\cdot||$ denote the absolute value and the standard Euclidean norm, respectively. We denote the nonnegative and positive orthants in Euclidean vector space of dimension K as $\mathbb{R}_+^K$ and $\mathbb{R}_{++}^K$. The notations $\boldsymbol{a}||\boldsymbol{b}$ and $\boldsymbol{a}\not\parallel\boldsymbol{b}$ denote that $\boldsymbol{a}$ is parallel to $\boldsymbol{b}$ and $\boldsymbol{a}$ is not parallel to $\boldsymbol{b}$, respectively. We denote $\boldsymbol{B} \succeq 0$ and $\boldsymbol{B} \succ 0$ as $\boldsymbol{B}$ being positive semi-definite and positive definite, respectively. The notation $\succeq_{\mathcal{K}}$ denotes the generalized inequality with respect to a second-order cone $\mathcal{K}$ as follows:

$$\begin{bmatrix} t \\ \boldsymbol{u} \end{bmatrix} \succeq_{\mathcal{K}} 0 \Leftrightarrow \|\boldsymbol{u}\| \le t.$$

We denote the primal optimization problem as $\mathcal{P}$, its associated dual optimization problem as $\mathcal{DP}$, and its associated robust counterpart as $\mathcal{RP}$.

II. System Model

A. Signal and Channel Models

We consider a wireless relay network consisting of $K+2$ single-antenna nodes: a designated source-destination node pair together with K relay nodes located randomly and independently in a domain of a fixed area. We consider a scenario in which there is no direct link between the source and destination nodes. All nodes operating in a common frequency band are in half-duplex mode, so transmission occurs over two time slots.

In the first time slot, all relay nodes receive the signal transmitted by the source node. After processing the received signals, the relay nodes transmit the processed data to the destination node during the second time slot in which the source node remains silent. We assume perfect synchronization at the destination node.[5] The received signals at the relay and destination nodes can then be written as

$$\boldsymbol{y}_{\mathrm{R}} = \boldsymbol{h}_{\mathrm{B}} x_{\mathrm{S}} + \boldsymbol{z}_{\mathrm{R}}, \quad \text{First slot} \tag{1}$$

$$y_{\mathrm{D}} = \boldsymbol{h}_{\mathrm{F}}^T \boldsymbol{x}_{\mathrm{R}} + z_{\mathrm{D}} \quad \text{Second slot} \tag{2}$$

where x_{S} is the transmitted signal from the source node to the relay nodes, $\boldsymbol{x}_{\mathrm{R}}$ is the $K \times 1$ transmitted signal vector from the relay nodes to the destination node, $\boldsymbol{y}_{\mathrm{R}}$ is the $K \times 1$ received signal vector at the relay nodes, y_{D} is the received signal at the destination node, $\boldsymbol{z}_{\mathrm{R}} \sim \tilde{\mathcal{N}}_K(\mathbf{0}, \boldsymbol{\Sigma}_{\mathrm{R}})$ is the $K \times 1$ noise vector at the relay nodes, and $z_{\mathrm{D}} \sim \tilde{\mathcal{N}}(0, \sigma_{\mathrm{D}}^2)$ is the noise at the destination node.[6] Note that the different noise variances at the relay nodes are reflected in $\boldsymbol{\Sigma}_{\mathrm{R}} \triangleq \mathrm{diag}(\sigma_{\mathrm{R},1}^2, \ldots, \sigma_{\mathrm{R},K}^2)$. Moreover, $\boldsymbol{z}_{\mathrm{R}}$ and z_{D} are independent and are mutually uncorrelated with x_{S} and $\boldsymbol{x}_{\mathrm{R}}$. The $K \times 1$ random channel vectors from source to relay and from relay to destination are respectively denoted by $\boldsymbol{h}_{\mathrm{B}} = [h_{\mathrm{B},1}, \ldots, h_{\mathrm{B},K}]^T \in \mathbb{C}^K$ and $\boldsymbol{h}_{\mathrm{F}} = [h_{\mathrm{F},1}, \ldots, h_{\mathrm{F},K}]^T \in \mathbb{C}^K$. For convenience, we shall refer to $\boldsymbol{h}_{\mathrm{B}}$ as the backward channel and $\boldsymbol{h}_{\mathrm{F}}$ as the forward channel.

In general, we can decompose each instantaneous element in $\boldsymbol{h}_{\mathrm{B}}$ and $\boldsymbol{h}_{\mathrm{F}}$ into the product of two different fading effects with different timescales [19]. Specifically, we can write

$$h_{\mathrm{B},k} = \alpha_{\mathrm{B},k} \sqrt{S_{\mathrm{B},k}} \tag{3}$$

$$h_{\mathrm{F},k} = \alpha_{\mathrm{F},k} \sqrt{S_{\mathrm{F},k}} \tag{4}$$

[1]Exactly how this global CSI can be obtained by the central unit is beyond the scope of this paper.

[2]In this way, we do not require very frequent power updates, which leads to significant power savings.

[3]The required QoS is considered to be satisfied when the output signal-to-noise ratio (SNR) at the destination node exceeds a given target value.

[4]Such an approach is akin to a slow adaptive modulation technique that adapts constellation size to the slow variations of the channels [18].

[5]Exactly how to achieve this synchronization or the effect of synchronization errors on performance is beyond the scope of this paper.

[6]$\tilde{\mathcal{N}}(\mu, \sigma_2)$ denotes a complex circularly symmetric Gaussian distribution with mean μ and variance σ^2. Similarly, $\tilde{\mathcal{N}}_K(\boldsymbol{\mu}, \boldsymbol{\Sigma})$ denotes a complex K-variate Gaussian distribution with a mean vector $\boldsymbol{\mu}$ and a covariance matrix $\boldsymbol{\Sigma}$.

where $\alpha_{\mathrm{B},k} \in \mathbb{C}$ and $\alpha_{\mathrm{F},k} \in \mathbb{C}$ reflect the channel gain associated with small-scale fading from the source to the kth relay and the kth relay to the destination, respectively. Such small-scale fading is typically due to local scattering of the environment and varies with a timescale on the order of milliseconds, and we can model $\alpha_{\mathrm{B},k} \sim \tilde{\mathcal{N}}(0,1)$ and $\alpha_{\mathrm{F},k} \sim \tilde{\mathcal{N}}(0,1)$ for all k. Each is assumed to be independent across all the relay nodes.[7] On the other hand, $S_{\mathrm{B},k} \in \mathbb{R}_{+}$ and $S_{\mathrm{F},k} \in \mathbb{R}_{+}$ capture the large-scale fading effects that are caused by shadowing. Large-scale fading varies with a timescale on the order of seconds. Usually, we can model $S_{\mathrm{B},k}$ and $S_{\mathrm{F},k}$ as [19]

$$S_{\mathrm{B},k} = \frac{10^{\sigma_{\mathrm{dB}} N/10}}{d_{\mathrm{B},k}^{\varepsilon}} \tag{5}$$

$$S_{\mathrm{F},k} = \frac{10^{\sigma_{\mathrm{dB}} N/10}}{d_{\mathrm{F},k}^{\varepsilon}} \tag{6}$$

where $d_{\mathrm{B},k}$ and $d_{\mathrm{F},k}$ are the normalized distances from the kth relay to the source and destination, respectively, ε is the path-loss exponent which corresponds to a decay in power, σ_{dB} is the standard deviation of the log-normal shadowing in dB, and N is a real Gaussian random variable (r.v.) such that $N \sim \mathcal{N}(0,1)$.[8]

At the source node, we impose an individual source power constraint P_{S}, such that $Q_{\mathrm{S}} \triangleq \mathbb{E}\{|x_{\mathrm{S}}|^2\} \leq P_{\mathrm{S}}$. Similarly, at the relay nodes, we impose an individual relay power constraint P such that $p_k \triangleq [\boldsymbol{Q}_{\mathrm{R}}]_{k,k} \leq P$ for $k = 1, \ldots, K$, where $\boldsymbol{Q}_{\mathrm{R}} \triangleq \mathbb{E}\{\boldsymbol{x}_{\mathrm{R}}\boldsymbol{x}_{\mathrm{R}}^{\dagger}|\boldsymbol{h}_{\mathrm{B}}\}$ and p_k is the transmission power allocated to the kth relay node.

For AF relaying, the relay nodes simply transmit scaled versions of their received signals while satisfying power constraints. In this case, $\boldsymbol{x}_{\mathrm{R}}$ in (2) is given by

$$\boldsymbol{x}_{\mathrm{R}} = \boldsymbol{G}\boldsymbol{y}_{\mathrm{R}} \tag{7}$$

where $\boldsymbol{G}$ denotes the $K \times K$ diagonal relay gain matrix, and $\boldsymbol{Q}_{\mathrm{R}}$ becomes[9]

$$\boldsymbol{Q}_{\mathrm{R}} = \boldsymbol{G}\left(P_{\mathrm{S}}\boldsymbol{h}_{\mathrm{B}}\boldsymbol{h}_{\mathrm{B}}^{\dagger} + \boldsymbol{\Sigma}_{\mathrm{R}}\right)\boldsymbol{G}^{\dagger}. \tag{8}$$

The diagonal structure of $\boldsymbol{G}$ ensures that each relay node does not require knowledge about the signals at other relay nodes. For noncoherent AF relaying, the kth diagonal element of $\boldsymbol{G}$ is given by [21], [22]

$$g_{\mathrm{noncoh}}^{(k)} = \sqrt{\beta_k p_k} \tag{9}$$

[7]The independence assumption arises due to the presence of different propagation paths and scatterers for each relay node.

[8]The parameter ε is environment-dependent and can approximately range from 1.6 (e.g., hallways inside buildings) to 8 (e.g., dense urban environments), where $\varepsilon = 2$ corresponds to the free space propagation [20]. On the other hand, the typical values of σ_{dB} range from 4 to 13 dB for outdoor channels [20]. For ease of exposition, we have assumed that the attenuations due to shadowing are independent and identically distributed (i.i.d.).

[9]Note that in (8), the source employs maximum allowable power P_{S} in order to maximize the SNR at the destination node.

where $\beta_k = 1/(P_{\mathrm{S}}S_{\mathrm{B},k}^2 + \sigma_{\mathrm{R},k}^2)$. On the other hand, if each relay node can track the phases of the small-scale fading associated with both backward and forward channels, it can perform distributed beamforming. This is referred to as coherent AF relaying, and the kth diagonal element of $\boldsymbol{G}$ is given by [23], [24]

$$g_{\mathrm{coh}}^{(k)} = \sqrt{\beta_k p_k}\frac{\alpha_{\mathrm{B},k}^{*}}{|\alpha_{\mathrm{B},k}|}\frac{\alpha_{\mathrm{F},k}^{*}}{|\alpha_{\mathrm{F},k}|}. \tag{10}$$

It follows from (1), (2) and (7) that the received signal at the destination node can be written as

$$y_{\mathrm{D}} = \boldsymbol{h}_{\mathrm{F}}^{T}\boldsymbol{G}\boldsymbol{h}_{\mathrm{B}}x_{\mathrm{S}} + \underbrace{\boldsymbol{h}_{\mathrm{F}}^{T}\boldsymbol{G}\boldsymbol{z}_{\mathrm{R}} + z_{\mathrm{D}}}_{\triangleq \tilde{z}_{\mathrm{D}}} \tag{11}$$

where $\tilde{z}_{\mathrm{D}}$ represents the effective noise at the destination node, and the instantaneous SNR at the destination node conditioned on $\boldsymbol{h}_{\mathrm{B}}$ and $\boldsymbol{h}_{\mathrm{F}}$ is then given by

$$\mathsf{SNR}(\boldsymbol{p}) = \frac{P_{\mathrm{S}}\boldsymbol{h}_{\mathrm{F}}^{T}\boldsymbol{G}\boldsymbol{h}_{\mathrm{B}}\boldsymbol{h}_{\mathrm{B}}^{\dagger}\boldsymbol{G}^{\dagger}\boldsymbol{h}_{\mathrm{F}}^{*}}{\boldsymbol{h}_{\mathrm{F}}^{T}\boldsymbol{G}\boldsymbol{\Sigma}_{\mathrm{R}}\boldsymbol{G}^{\dagger}\boldsymbol{h}_{\mathrm{F}}^{*} + \sigma_{\mathrm{D}}^2} \tag{12}$$

where $\boldsymbol{p} = [p_1, \ldots, p_K]^T$ denotes the vector of transmitted powers of the relay nodes.

B. Problem Formulation

Given instantaneous $\boldsymbol{h}_{\mathrm{B}}$ and $\boldsymbol{h}_{\mathrm{F}}$ at the destination node, we formulate the relay power allocation problem for minimizing the total relay transmission power subject to the constraint on SNR at the destination node. This constraint is equivalent to a certain QoS requirement such as the bit error rate or outage probability, where QoS is satisfied when the SNR at the destination node exceeds a given target value γ_{th}. With this QoS constraint, we can mathematically formulate the optimization problem as

$$\begin{aligned}\mathcal{P}_{\mathsf{SNR}}(\gamma_{\mathrm{th}}): \min\nolimits_{\boldsymbol{p}}\ & \mathrm{tr}(\boldsymbol{Q}_{\mathrm{R}}) \\ \text{s.t.}\ & \gamma_{\mathrm{th}} \leq \mathsf{SNR}(\boldsymbol{p}) \\ & 0 \leq [\boldsymbol{Q}_{\mathrm{R}}]_{k,k} \leq P,\ \forall k \in \{1, \ldots, K\}\end{aligned} \tag{13}$$

where the last constraint in (13) captures the fact that relay transmission power in practical systems cannot be arbitrarily large.[10] Note that solving the program $\mathcal{P}_{\mathsf{SNR}}(\gamma_{\mathrm{th}})$ in (13) requires the instantaneous values of $\boldsymbol{h}_{\mathrm{B}}$ and $\boldsymbol{h}_{\mathrm{F}}$.

Due to the timescale associated with small-scale fading, frequent communication between the relay nodes and the central unit is required to determine new power allocations. This motivates practical algorithms that track only large-scale fading. One possible approach is to adopt the certainty-equivalent (CE) formulation, which was developed in the context of power control for cellular networks [25], [26]. In our context, the CE output SNR for noncoherent AF relaying can be written as

$$\mathsf{SNR}_{\mathrm{noncoh}}^{\mathrm{CE}}(\boldsymbol{p}) = \frac{P_{\mathrm{S}}\sum_{k=1}^{K}\beta_k S_{\mathrm{B},k}S_{\mathrm{F},k}p_k}{\sum_{k=1}^{K}\beta_k S_{\mathrm{F},k}\sigma_{\mathrm{R},k}^2 p_k + \sigma_{\mathrm{D}}^2} \tag{14}$$

[10]Note that in conventional QoS formulation, the last constraint in (13) is omitted, hence it is guaranteed to be feasible in the absence of CSI uncertainties.

where we have replaced all r.v.'s associated with $\{\alpha_{\mathrm{F},k}\}_{k=1}^K$ and $\{\alpha_{\mathrm{B},k}\}_{k=1}^K$ in (12) with their expected values. For coherent AF relaying, we approximate the CE output SNR as

$$\mathsf{SNR}_{\mathrm{coh}}^{\mathrm{CE}}(\boldsymbol{p}) \approx \frac{P_{\mathrm{S}}\left(\sum_{k=1}^K \sqrt{\beta_k S_{\mathrm{B},k} S_{\mathrm{F},k} p_k}\right)^2}{\sum_{k=1}^K \beta_k S_{\mathrm{F},k}\sigma_{\mathrm{R},k}^2 p_k + \sigma_{\mathrm{D}}^2}. \tag{15}$$

Indeed, (15) is an upper bound of the actual CE output SNR. We choose to use this expression in (15) since it allows efficient formulation for the optimization problem. Substituting (14) and (15) into (13), we can now design power allocation algorithms that track only large-scale fading. However, these slow power allocations may lead to undesirably high outage probability, i.e., $\mathbb{P}\{\mathsf{SNR}(\boldsymbol{p}) < \gamma_{\mathrm{th}}\}$, due to the random fluctuations caused by small-scale fading. This can be alleviated by using a larger SNR target value to allow for fade margins [26]–[28].[11] In our case, this corresponds to using a target value $\gamma_{\mathrm{th}}^{\mathrm{CE}} = \kappa\gamma_{\mathrm{th}}$ with $\kappa > 1$, where we refer to $\gamma_{\mathrm{th}}^{\mathrm{CE}}$ as the CE SNR target value.[12]

III. Optimal Relay Power Allocation

In this section, we consider the power optimization problems subject to CE SNR constraints for both noncoherent and coherent AF relay networks.

A. Noncoherent Amplify-and-Forward Relay Network

Let $\boldsymbol{d} = [d_1, \ldots, d_K]^T \in \mathbb{R}_+^K$ and $\boldsymbol{e} = [e_1, \ldots, e_K]^T \in \mathbb{R}_+^K$ where

$$d_k = \frac{\sigma_{\mathrm{R},k}^2}{\sigma_{\mathrm{D}}^2}\beta_k S_{\mathrm{F},k} \tag{16}$$

$$e_k = \beta_k S_{\mathrm{F},k} S_{\mathrm{B},k}. \tag{17}$$

The CE power optimization problem for the noncoherent AF relay network can be formulated as

$$\begin{aligned} \mathcal{P}_{\mathrm{noncoh}}^{\mathrm{CE}}\left(\gamma_{\mathrm{th}}^{\mathrm{CE}}\right) : \min_{\boldsymbol{p}} \quad & \sum_{k=1}^K p_k \\ \text{s.t.} \quad & \gamma_{\mathrm{th}}^{\mathrm{CE}} \le \frac{P_{\mathrm{S}}}{\sigma_{\mathrm{D}}^2}\frac{\boldsymbol{e}^T\boldsymbol{p}}{\boldsymbol{d}^T\boldsymbol{p}+1} \\ & \boldsymbol{p} \in \mathcal{X}_p \end{aligned} \tag{18}$$

where $\mathcal{X}_p = \{\boldsymbol{p} \in \mathbb{R}^K : 0 \le p_k \le P, \forall k \in \{1, \ldots, K\}\}$. Note that the above program only requires perfect knowledge of large-scale fading.

Theorem 1: The program $\mathcal{P}_{\mathrm{noncoh}}^{\mathrm{CE}}(\gamma_{\mathrm{th}}^{\mathrm{CE}})$ is a linear program given by

$$\begin{aligned} \min_{\boldsymbol{p}} \quad & \mathbf{1}^T\boldsymbol{p} \\ \text{s.t.} \quad & \boldsymbol{m} \ge \boldsymbol{B}\boldsymbol{p} \end{aligned} \tag{19}$$

where $\boldsymbol{B} \in \mathbb{R}^{(2K+1)\times K}$ and $\boldsymbol{m} \in \mathbb{R}^{2K+1}$ are given by

$$\boldsymbol{B} = \begin{bmatrix} \boldsymbol{d}^T - \frac{P_{\mathrm{S}}}{\gamma_{\mathrm{th}}^{\mathrm{CE}}\sigma_{\mathrm{D}}^2}\boldsymbol{e}^T \\ \boldsymbol{I}_K \\ -\boldsymbol{I}_K \end{bmatrix}, \quad \boldsymbol{m} = \begin{bmatrix} -1 \\ P\mathbf{1} \\ \mathbf{0} \end{bmatrix}. \tag{20}$$

When the problem is feasible, there exists a set of optimal solutions $\{\boldsymbol{p}_{\mathrm{opt}}\}$ when $-\mathbf{1}\|\boldsymbol{b}_1$, and a unique optimal solution $\boldsymbol{p}_{\mathrm{opt}}$ when $-\mathbf{1} \not\parallel \boldsymbol{b}_1$, such that $\boldsymbol{b}_1 = \boldsymbol{d} - (P_{\mathrm{S}}/\gamma_{\mathrm{th}}^{\mathrm{CE}}\sigma_{\mathrm{D}}^2)\boldsymbol{e}$.

Proof: To show that $\mathcal{P}_{\mathrm{noncoh}}^{\mathrm{CE}}(\gamma_{\mathrm{th}}^{\mathrm{CE}})$ is an LP, we simply express the CE SNR constraint and the power constraints in the form of $\boldsymbol{b}_k^T\boldsymbol{p} \le m_k$, where $\boldsymbol{b}_k^T$ is the kth row vector of the matrix $\boldsymbol{B}$ and m_k is the kth element of the vector $\boldsymbol{m}$ defined in (20). Since the objective function is linear in $\boldsymbol{p}$ and the feasible set is a polyhedron, it follows that we have an LP, as shown in (19). When the problem is feasible, the polyhedron is non-empty and the optimal objective value is finite. Furthermore, the polyhedron is bounded since it is contained in a hypercube. From [29, Corollary 2.2], it follows that there is at least one extreme point in the polyhedron. Therefore, there exists at least one optimal solution for program $\mathcal{P}_{\mathrm{noncoh}}^{\mathrm{CE}}(\gamma_{\mathrm{th}}^{\mathrm{CE}})$ [29, Theorem 2.8]. Note that the uniqueness of the optimal solution depends on the direction of $\boldsymbol{b}_1$. Since the objective function is to minimize $\mathbf{1}^T\boldsymbol{p}$, the optimal solution is to travel as far as possible in the $-\mathbf{1}$ direction. However, when $-\mathbf{1}\|\boldsymbol{b}_1$, the set of optimal solutions lies along the hyperplane $\boldsymbol{b}_1^T\boldsymbol{p} = m_1$ as this is the boundary of the feasible set. On the other hand, when $-\mathbf{1} \not\parallel \boldsymbol{b}_1$, there is a unique optimal solution that can be found by moving in the $-\mathbf{1}$ direction. □

Remark 1: To verify the feasibility of $\mathcal{P}_{\mathrm{noncoh}}^{\mathrm{CE}}(\gamma_{\mathrm{th}}^{\mathrm{CE}})$, we consider the following simple LP:

$$\begin{aligned} \min_{\boldsymbol{p},t} \quad & t \\ \text{s.t.} \quad & \boldsymbol{m} + t\mathbf{1} \ge \boldsymbol{B}\boldsymbol{p} \end{aligned} \tag{21}$$

where $t \in \mathbb{R}$. It is clear that the program $\mathcal{P}_{\mathrm{noncoh}}^{\mathrm{CE}}(\gamma_{\mathrm{th}}^{\mathrm{CE}})$ is feasible when $t_{\mathrm{opt}} \le 0$, where t_{opt} is the optimal solution to the LP in (21). Since LP can be solved very easily with simplex algorithm, we can also use (21) to determine $\gamma_{\mathrm{th}}^{\mathrm{CE}}$ that corresponds to $t_{\mathrm{opt}} \le 0$. Such $\gamma_{\mathrm{th}}^{\mathrm{CE}}$ will result in feasible program $\mathcal{P}_{\mathrm{noncoh}}^{\mathrm{CE}}(\gamma_{\mathrm{th}}^{\mathrm{CE}})$.

Theorem 2 (Duality): The dual problem of $\mathcal{P}_{\mathrm{noncoh}}^{\mathrm{CE}}(\gamma_{\mathrm{th}}^{\mathrm{CE}})$ is given by

$$\begin{aligned} \mathcal{DP}_{\mathrm{noncoh}}^{\mathrm{CE}}\left(\gamma_{\mathrm{th}}^{\mathrm{CE}}\right) : \max_{\boldsymbol{\nu}} \quad & -\boldsymbol{m}^T\boldsymbol{\nu} \\ \text{s.t.} \quad & \boldsymbol{B}^T\boldsymbol{\nu} + \mathbf{1} = \mathbf{0} \end{aligned} \tag{22}$$

where $\boldsymbol{\nu} \in \mathbb{R}_+^{2K+1}$ is the dual feasible variable. Since strong duality holds when either the primal or dual problems is feasible, there exists an optimal $\boldsymbol{\nu}_{\mathrm{opt}} \in \mathbb{R}_+^{2K+1}$ such that

$$\begin{aligned} \mathbf{1}^T\boldsymbol{p}_{\mathrm{opt}} + \boldsymbol{m}^T\boldsymbol{\nu}_{\mathrm{opt}} &= 0 \\ \boldsymbol{B}^T\boldsymbol{\nu}_{\mathrm{opt}} + \mathbf{1} &= \mathbf{0}. \end{aligned} \tag{23}$$

Proof: See Appendix I. □

[11] Note that this also compensates for the use of approximation in (15).

[12] Clearly, κ depends on the types of relaying scheme. For convenience, we use the same notation κ for both noncoherent and coherent AF relay networks.

B. Coherent Amplify-and-Forward Relay Network

Let $\boldsymbol{A} = \mathrm{diag}(a_1, \ldots, a_K) \in \mathbb{R}_+^{K \times K}$ and $\boldsymbol{c} = [c_1, \ldots, c_K]^T \in \mathbb{R}_+^K$ where

$$a_k = \frac{\sigma_{\mathrm{R},k}}{\sigma_{\mathrm{D}}} \sqrt{\beta_k S_{\mathrm{F},k}} \tag{24}$$

$$c_k = \sqrt{\beta_k S_{\mathrm{F},k} S_{\mathrm{B},k}}. \tag{25}$$

The CE power optimization problem for the coherent AF relay network can be formulated as

$$\begin{aligned} \mathcal{P}_{\mathrm{coh}}^{\mathrm{CE}}\left(\gamma_{\mathrm{th}}^{\mathrm{CE}}\right) : \min_{\boldsymbol{\zeta}} \quad & \sum_{k=1}^{K} \zeta_k^2 \\ \text{s.t.} \quad & \gamma_{\mathrm{th}}^{\mathrm{CE}} \le \frac{P_{\mathrm{S}}}{\sigma_{\mathrm{D}}^2} \frac{(\boldsymbol{c}^T \boldsymbol{\zeta})^2}{\|\boldsymbol{A}\boldsymbol{\zeta}\|^2 + 1} \\ & \boldsymbol{\zeta} \in \mathcal{X}_{\zeta} \end{aligned} \tag{26}$$

where $\zeta_k = \sqrt{p_k}$ for all k and $\mathcal{X}_{\zeta} = \{\boldsymbol{\zeta} \in \mathbb{R}^K : 0 \le \zeta_k \le \sqrt{P}, \forall k \in \{1, \ldots, K\}\}$.[13]

Theorem 3: The program $\mathcal{P}_{\mathrm{coh}}^{\mathrm{CE}}(\gamma_{\mathrm{th}}^{\mathrm{CE}})$ is a strictly convex optimization program with a compact feasible set. When the problem is feasible, there exists a unique optimal solution $\boldsymbol{\zeta}_{\mathrm{opt}}$. We can equivalently formulate $\mathcal{P}_{\mathrm{coh}}^{\mathrm{CE}}(\gamma_{\mathrm{th}}^{\mathrm{CE}})$ in SOCP form as[14]

$$\begin{aligned} \min_{\boldsymbol{\zeta},t} \quad & t \\ \text{s.t.} \quad & \begin{bmatrix} \boldsymbol{c}^T \boldsymbol{\zeta} \sqrt{\frac{P_{\mathrm{S}}}{\gamma_{\mathrm{th}}^{\mathrm{CE}} \sigma_{\mathrm{D}}^2}} \\ \begin{pmatrix} 1 \\ \boldsymbol{A}\boldsymbol{\zeta} \end{pmatrix} \end{bmatrix} \succeq_{\mathcal{K}} 0 \\ & \begin{bmatrix} \frac{t+1}{2} \\ \begin{pmatrix} \boldsymbol{\zeta} \\ \frac{t-1}{2} \end{pmatrix} \end{bmatrix} \succeq_{\mathcal{K}} 0 \\ & \boldsymbol{\zeta} \in \mathcal{X}_{\zeta}. \end{aligned} \tag{27}$$

Proof: Clearly, the objective function $\|\boldsymbol{\zeta}\|^2$ is a strictly convex function since the Hessian matrix of the objective function is positive definite [31], [32]. To show that the feasible set is convex, we cast the first constraint in (26) in standard form as follows:

$$\boldsymbol{c}^T \boldsymbol{\zeta} \sqrt{\frac{P_{\mathrm{S}}}{\gamma_{\mathrm{th}}^{\mathrm{CE}} \sigma_{\mathrm{D}}^2}} \ge \left\| \begin{pmatrix} 1 \\ \boldsymbol{A}\boldsymbol{\zeta} \end{pmatrix} \right\| \tag{28}$$

which can be rewritten in the form of an SOC constraint as

$$\begin{bmatrix} \boldsymbol{c}^T \boldsymbol{\zeta} \sqrt{\frac{P_{\mathrm{S}}}{\gamma_{\mathrm{th}}^{\mathrm{CE}} \sigma_{\mathrm{D}}^2}} \\ \begin{pmatrix} 1 \\ \boldsymbol{A}\boldsymbol{\zeta} \end{pmatrix} \end{bmatrix} \succeq_{\mathcal{K}} 0. \tag{29}$$

Therefore, the feasible set in (26) is convex since it is the intersection of a hypercube and an SOC, which are both convex sets [31], [32]. As a result, $\mathcal{P}_{\mathrm{coh}}^{\mathrm{CE}}(\gamma_{\mathrm{th}}^{\mathrm{CE}})$ is a strictly convex optimization program. Moreover, the feasible set is bounded since it is contained in a hypercube. It is also closed since it consists of the intersection of an SOC and a hypercube, which are both closed sets [31], [32]. Therefore, it follows that the feasible set is compact. By the Weierstrass theorem, it follows that there exists at least one optimal solution for program $\mathcal{P}_{\mathrm{coh}}^{\mathrm{CE}}(\gamma_{\mathrm{th}}^{\mathrm{CE}})$ [31], [32]. Furthermore, given the strict convexity of $\|\boldsymbol{\zeta}\|^2$, there is a unique optimal solution $\boldsymbol{\zeta}_{\mathrm{opt}}$.

To cast $\mathcal{P}_{\mathrm{coh}}^{\mathrm{CE}}(\gamma_{\mathrm{th}}^{\mathrm{CE}})$ into an SOCP, we use a slack variable $t \in \mathbb{R}_+$. The program can be equivalently written as[15]

$$\begin{aligned} \min_{\boldsymbol{\zeta},t} \quad & t \\ \text{s.t.} \quad & \begin{bmatrix} \boldsymbol{c}^T \boldsymbol{\zeta} \sqrt{\frac{P_{\mathrm{S}}}{\gamma_{\mathrm{th}}^{\mathrm{CE}} \sigma_{\mathrm{D}}^2}} \\ \begin{pmatrix} 1 \\ \boldsymbol{A}\boldsymbol{\zeta} \end{pmatrix} \end{bmatrix} \succeq_{\mathcal{K}} 0 \\ & \sum_{k=1}^{K} \zeta_k^2 \le t \\ & \boldsymbol{\zeta} \in \mathcal{X}_{\zeta}. \end{aligned} \tag{30}$$

From [30], we can easily express the second constraint in (30) as

$$\begin{bmatrix} \frac{t+1}{2} \\ \begin{pmatrix} \boldsymbol{\zeta} \\ \frac{t-1}{2} \end{pmatrix} \end{bmatrix} \succeq_{\mathcal{K}} 0. \tag{31}$$

Substituting (31) into (30), we obtain the program (27) in SOCP form. □

Proposition 1 (Feasibility): A necessary and sufficient condition for $\mathcal{P}_{\mathrm{coh}}^{\mathrm{CE}}(\gamma_{\mathrm{th}}^{\mathrm{CE}})$ to be feasible is given by

$$\frac{\gamma_{\mathrm{th}}^{\mathrm{CE}} \sigma_{\mathrm{D}}^2}{P_{\mathrm{S}}} \le \Upsilon_{\mathrm{opt}} \tag{32}$$

where Υ_{opt} is the optimal objective value of the following maximization problem:

$$\begin{aligned} \max_{\boldsymbol{\zeta}} \quad & \frac{(\boldsymbol{c}^T \boldsymbol{\zeta})^2}{\|\boldsymbol{A}\boldsymbol{\zeta}\|^2 + 1} \\ \text{s.t.} \quad & \boldsymbol{\zeta} \in \mathcal{X}_{\zeta}. \end{aligned} \tag{33}$$

Furthermore, we can derive a necessary condition given by

$$\gamma_{\mathrm{th}}^{\mathrm{CE}} < \frac{P_{\mathrm{S}} \|\boldsymbol{c}\|^2}{\sigma_{\mathrm{D}}^2 \tau_{\min}(\boldsymbol{A}^T \boldsymbol{A})} \tag{34}$$

where $\tau_{\min}(\boldsymbol{A}^T \boldsymbol{A})$ denotes the smallest eigenvalue of $\boldsymbol{A}^T \boldsymbol{A}$, and $\tau_{\min}(\boldsymbol{A}^T \boldsymbol{A}) = \min_{1 \le k \le K} a_k^2$.

Proof: See Appendix II. □

Remark 2: Proposition 1 provides us with useful conditions not only for verifying the feasibility of $\mathcal{P}_{\mathrm{coh}}^{\mathrm{CE}}(\gamma_{\mathrm{th}}^{\mathrm{CE}})$, but also for designing system parameters such as P_{S}, $\gamma_{\mathrm{th}}^{\mathrm{CE}}$, and K. For example, we could use the simple condition in (34) to check if $\mathcal{P}_{\mathrm{coh}}^{\mathrm{CE}}(\gamma_{\mathrm{th}}^{\mathrm{CE}})$ is infeasible. We check the condition in (32) only when (34) is satisfied. When (32) or (34) fails, we adjust the

[13]Similarly, the above program only requires perfect knowledge of large-scale fading.

[14]The SOCP form can be solved efficiently [30].

[15]Note that there is no loss of optimality by introducing such a slack variable [31], [32].

system parameters to ensure that both (32) and (34) are satisfied. This process effectively converts an infeasible program into a feasible one.

As for the case of the noncoherent AF relay network, we formulate the dual problem of (26) and derive its Karush-Kuhn-Tucker (KKT) conditions in the following theorem.

Theorem 4 (Duality): The dual problem of $\mathcal{P}_{\rm coh}^{\rm CE}(\gamma_{\rm th}^{\rm CE})$ is given by

$$\mathcal{DP}_{\rm coh}^{\rm CE}\left(\gamma_{\rm th}^{\rm CE}\right) : \max_{\mu,\boldsymbol{\lambda},\boldsymbol{\nu}} g(\mu,\boldsymbol{\lambda},\boldsymbol{\nu}) \quad \text{s.t.} \quad \boldsymbol{I}_K + \mu\boldsymbol{Q} \succ 0 \tag{35}$$

with

$$\begin{aligned} g(\mu,\boldsymbol{\lambda},\boldsymbol{\nu}) &= \frac{\mu\gamma_{\rm th}^{\rm CE}\sigma_{\rm D}^2}{P_{\rm S}} - {\rm tr}(\boldsymbol{\Lambda}) \\ &\quad - \frac{1}{4}(\boldsymbol{\lambda}-\boldsymbol{\nu})^T(\boldsymbol{I}_K+\mu\boldsymbol{Q})^{-1}(\boldsymbol{\lambda}-\boldsymbol{\nu}) \\ \boldsymbol{Q} &= \frac{\gamma_{\rm th}^{\rm CE}\sigma_{\rm D}^2}{P_{\rm S}}\boldsymbol{A}^T\boldsymbol{A} - \boldsymbol{c}\boldsymbol{c}^T \\ \boldsymbol{\Lambda} &= \sqrt{P}{\rm diag}(\lambda_1,\ldots,\lambda_K) \end{aligned}$$

where $\mu \in \mathbb{R}_+$, $\boldsymbol{\lambda} \in \mathbb{R}_+^K$ and $\boldsymbol{\nu} \in \mathbb{R}_+^K$ are the dual feasible variables. If the primal problem is strictly feasible, strong duality holds and there exists $\mu > 0$ such that

$$\mu > -\frac{1}{\tau_{\min}(\boldsymbol{Q})}. \tag{36}$$

Moreover, the optimal primal solution $\boldsymbol{\zeta}_{\rm opt}$ takes the form

$$\boldsymbol{\zeta}_{\rm opt} = -\frac{1}{2}(\boldsymbol{I}_K + \mu_{\rm opt}\boldsymbol{Q})^{-1}(\boldsymbol{\lambda}_{\rm opt} - \boldsymbol{\nu}_{\rm opt}) \tag{37}$$

where $(\mu_{\rm opt}, \boldsymbol{\lambda}_{\rm opt}, \boldsymbol{\nu}_{\rm opt})$ is the optimal dual solution and $\mu_{\rm opt}$ satisfies the condition in (36).

Proof: See Appendix III. □

IV. Robust Relay Power Allocation

To account for CSI uncertainties, we adopt a robust optimization methodology [33], [34]. Specifically, this methodology treats uncertainty by assuming that CSI is a deterministic variable within a bounded set of possible values. The size of the uncertainty set corresponds to the amount of uncertainty about the CSI.[16] This methodology ensures that the robust counterparts of our optimization problems lead to feasible solutions and yield good performance in all realizations of CSI within the uncertainty set. As in [33], [34], we consider an ellipsoidal uncertainty set for simplicity.[17]

[16]The singleton uncertainty set corresponds to the case of perfect CSI.

[17]Besides resulting in mathematical simplification, the ellipsoidal uncertainty set is well-motivated by practical CSI error models [35]. The size of the ellipsoidal uncertainty set can be known *a priori* from preliminary knowledge of the imperfect CSI estimation and/or from extensive wireless channel measurement campaigns.

A. Noncoherent Amplify-and-Forward Relay Network

In the following theorem, we formulate the robust counterpart of $\mathcal{P}_{\rm noncoh}^{\rm CE}(\gamma_{\rm th}^{\rm CE})$ with uncertainties in $\boldsymbol{d}$ and $\boldsymbol{e}$.

Theorem 5: Let $\mathcal{U}$ be an ellipsoidal uncertainty set given by

$$\mathcal{U} = \left\{ \boldsymbol{\Delta}(\boldsymbol{d},\boldsymbol{e}) = \boldsymbol{\Delta}_0 + \sum_{j=1}^{N_\Delta} w_j \boldsymbol{\Delta}_j : \|\boldsymbol{w}\| \le \rho_0 \right\} \tag{38}$$

where $\boldsymbol{\Delta}_j \triangleq (P_{\rm S}/\gamma_{\rm th}^{\rm CE}\sigma_{\rm D}^2)\boldsymbol{e}_j - \boldsymbol{d}_j \in \mathbb{R}^K$ and N_Δ is the dimension of $\boldsymbol{w}$. The robust counterpart of $\mathcal{P}_{\rm noncoh}^{\rm CE}(\gamma_{\rm th}^{\rm CE})$ with uncertainty set $\mathcal{U}$ is equivalent to the following SOCP:

$$\mathcal{RP}_{\rm noncoh}^{\rm CE}\left(\gamma_{\rm th}^{\rm CE}\right) : \min_{\boldsymbol{p}} \boldsymbol{1}^T\boldsymbol{p} \quad \text{s.t.} \quad \boldsymbol{p} \in \mathcal{S}_{\rm noncoh}\left(\gamma_{\rm th}^{\rm CE}\right) \tag{39}$$

where the feasible set $\mathcal{S}_{\rm noncoh}(\gamma_{\rm th}^{\rm CE})$ is given by

$$\mathcal{S}_{\rm noncoh}\left(\gamma_{\rm th}^{\rm CE}\right) = \left\{ \boldsymbol{p} \in \mathbb{R}^K : \begin{bmatrix} \frac{\boldsymbol{\Delta}_0^T\boldsymbol{p}-1}{\rho_0} \\ \breve{\boldsymbol{\Delta}} \end{bmatrix} \succeq_{\mathcal{K}} 0,\ \boldsymbol{p} \in \mathcal{X}_p \right\} \tag{40}$$

and $\breve{\boldsymbol{\Delta}} = \left[\boldsymbol{\Delta}_1^T\boldsymbol{p},\ldots,\boldsymbol{\Delta}_{N_\Delta}^T\boldsymbol{p}\right]^T$.

Proof: Since only $(\boldsymbol{d},\boldsymbol{e})$ in the first constraint of $\mathcal{P}_{\rm noncoh}^{\rm CE}(\gamma_{\rm th}^{\rm CE})$ is subject to uncertainty, we will focus on this constraint and build its robust counterpart, which is given by

$$\boldsymbol{e}^T\boldsymbol{p} \ge \frac{\gamma_{\rm th}^{\rm CE}\sigma_{\rm D}^2}{P_{\rm S}}(1 + \boldsymbol{d}^T\boldsymbol{p}) \tag{41}$$

for all $(\boldsymbol{d},\boldsymbol{e})$ that satisfy $\boldsymbol{\Delta}(\boldsymbol{d},\boldsymbol{e}) \in \mathcal{U}$. By substituting (38) into (41), we have equivalently

$$\breve{\boldsymbol{\Delta}}^T\boldsymbol{w} \ge -\left(\boldsymbol{\Delta}_0^T\boldsymbol{p} - 1\right), \quad \forall \boldsymbol{w} \in \{\boldsymbol{w} : \|\boldsymbol{w}\| \le \rho_0\} \tag{42}$$

and the robust constraint in (42) can be expressed as

$$\min_{\boldsymbol{w}:\|\boldsymbol{w}\|\le\rho_0} \{\breve{\boldsymbol{\Delta}}^T\boldsymbol{w}\} \ge -\left(\boldsymbol{\Delta}_0^T\boldsymbol{p} - 1\right). \tag{43}$$

By the Cauchy–Schwartz inequality, the minimum value on the left-hand side of (43) is equal to $-\rho_0\|\breve{\boldsymbol{\Delta}}\|$ and hence, we obtain an SOC constraint, as follows:

$$\begin{bmatrix} \frac{\boldsymbol{\Delta}_0^T\boldsymbol{p}-1}{\rho_0} \\ \breve{\boldsymbol{\Delta}} \end{bmatrix} \succeq_{\mathcal{K}} 0. \tag{44}$$

Since the objective function is linear in $\boldsymbol{p}$ and the rest of the constraints in (40) are linear constraints, it follows that $\mathcal{RP}_{\rm noncoh}^{\rm CE}(\gamma_{\rm th}^{\rm CE})$ is an SOCP. □

B. Coherent Amplify-and-Forward Relay Network

Similarly, we formulate the robust counterpart of $\mathcal{P}_{\rm coh}^{\rm CE}(\gamma_{\rm th}^{\rm CE})$ by incorporating uncertainties in $\boldsymbol{A}$ and $\boldsymbol{c}$ in the following theorem. Since $(\boldsymbol{A},\boldsymbol{c})$ appears only in the first constraint of (26), we need to simply focus on this constraint and build its robust counterpart given by

$$\boldsymbol{c}^T\boldsymbol{\zeta} \geq \sqrt{\frac{\gamma_{\rm th}^{\rm CE}\sigma_{\rm D}^2}{P_{\rm S}}\left(1+\|\boldsymbol{A}\boldsymbol{\zeta}\|^2\right)}, \quad \forall(\boldsymbol{A},\boldsymbol{c})\in\mathcal{U}. \tag{45}$$

In the following, we adopt a conservative approach which assumes that $\mathcal{U}$ affecting (45) is sidewise, i.e., the uncertainty affecting the right-hand side in (45) is independent of that affecting the left-hand side. Specifically, we have $\mathcal{U}=\mathcal{U}_{\rm R}\times\mathcal{U}_{\rm L}$. We summarize our results in the next theorem.

Theorem 6: Let $\mathcal{U}_{\rm R}$ and $\mathcal{U}_{\rm L}$ be sidewise independent ellipsoidal uncertainty sets given by

$$\mathcal{U}_{\rm R} = \left\{\boldsymbol{A}=\boldsymbol{A}_0+\sum_{j=1}^{N_A}u_j\boldsymbol{A}_j : \|\boldsymbol{u}\|\leq\rho_1\right\} \tag{46}$$

$$\mathcal{U}_{\rm L} = \left\{\boldsymbol{c}=\boldsymbol{c}_0+\sum_{j=1}^{N_c}v_j\boldsymbol{c}_j : \|\boldsymbol{v}\|\leq\rho_2\right\} \tag{47}$$

where N_A and N_c are the dimensions of $\boldsymbol{u}$ and $\boldsymbol{v}$, respectively. The approximate robust counterpart of $\mathcal{P}_{\rm coh}^{\rm CE}(\gamma_{\rm th}^{\rm CE})$ with uncertainty sets $\mathcal{U}_{\rm R}$ and $\mathcal{U}_{\rm L}$ can be written in SDP form:

$$\mathcal{RP}_{\rm coh}^{\rm CE}\left(\gamma_{\rm th}^{\rm CE}\right) : \min_{\boldsymbol{\zeta},t,\tau,\mu}\ t \quad \text{s.t.} \quad (\boldsymbol{\zeta},t,\tau,\mu)\in\mathcal{S}_{\rm coh}\left(\gamma_{\rm th}^{\rm CE}\right) \tag{48}$$

where $(\boldsymbol{\zeta},t,\tau,\mu)\in\mathbb{R}_+^K\times\mathbb{R}_+\times\mathbb{R}_+\times\mathbb{R}_+$ and the feasible set $\mathcal{S}_{\rm coh}(\gamma_{\rm th}^{\rm CE})$ is given by

$$\begin{aligned}\mathcal{S}_{\rm coh}\left(\gamma_{\rm th}^{\rm CE}\right) = \Bigg\{\boldsymbol{\zeta}\in\mathbb{R}_+^K : &\begin{bmatrix}\mu\boldsymbol{I}_{N_A} & \boldsymbol{0}_{N_A} & \breve{\boldsymbol{A}}^T\\ \boldsymbol{0}_{N_A}^T & \lambda-\mu\rho_1^2 & \boldsymbol{\zeta}^T\boldsymbol{A}_0^T\\ \breve{\boldsymbol{A}} & \boldsymbol{A}_0\boldsymbol{\zeta} & \lambda\boldsymbol{I}_K\end{bmatrix}\succeq 0\\ &\begin{bmatrix}\frac{(\boldsymbol{c}_0^T\boldsymbol{\zeta}-\tau)}{\rho_2}\boldsymbol{I}_{N_c} & \breve{\boldsymbol{c}}\\ \breve{\boldsymbol{c}}^T & \frac{(\boldsymbol{c}_0^T\boldsymbol{\zeta}-\tau)}{\rho_2}\end{bmatrix}\succeq 0\\ &\begin{bmatrix}\left(\frac{t+1}{2}\right)\boldsymbol{I}_{K+1} & \begin{pmatrix}\boldsymbol{\zeta}\\ \frac{t-1}{2}\end{pmatrix}\\ \begin{pmatrix}\boldsymbol{\zeta}^T & \frac{t-1}{2}\end{pmatrix} & \frac{t+1}{2}\end{bmatrix}\succeq 0\\ &\begin{bmatrix}\left(\frac{P+1}{2}\right)\boldsymbol{I}_2 & \begin{pmatrix}\zeta_k\\ \frac{P-1}{2}\end{pmatrix}\\ \begin{pmatrix}\zeta_k & \frac{P-1}{2}\end{pmatrix} & \frac{P+1}{2}\end{bmatrix}\succeq 0\\ &\begin{bmatrix}\tau & \sqrt{\frac{\gamma_{\rm th}^{\rm CE}\sigma_{\rm D}^2}{P_{\rm S}}}\\ \sqrt{\frac{\gamma_{\rm th}^{\rm CE}\sigma_{\rm D}^2}{P_{\rm S}}} & \tau\end{bmatrix}\succeq 0, \forall k\in\{1,\ldots,K\}\Bigg\}\end{aligned} \tag{49}$$

where $\lambda=\tau\sqrt{P_{\rm S}/\gamma_{\rm th}^{\rm CE}\sigma_{\rm D}^2}-1$, $\breve{\boldsymbol{A}}=[\boldsymbol{A}_1\boldsymbol{\zeta},\ldots,\boldsymbol{A}_{N_A}\boldsymbol{\zeta}]$, and $\breve{\boldsymbol{c}}=[\boldsymbol{c}_1^T\boldsymbol{\zeta},\ldots,\boldsymbol{c}_{N_c}^T\boldsymbol{\zeta}]^T$.

Proof: Due to the sidewise independence assumption, $\boldsymbol{\zeta}$ is robust feasible if there exists $\tau\in\mathbb{R}_+$ such that [36], [37]

$$\sqrt{\frac{\gamma_{\rm th}^{\rm CE}\sigma_{\rm D}^2}{P_{\rm S}}\left(1+\|\boldsymbol{A}\boldsymbol{\zeta}\|^2\right)}\leq\tau, \qquad \forall\boldsymbol{A}\in\mathcal{U}_{\rm R} \tag{50}$$

$$\tau\leq\boldsymbol{c}^T\boldsymbol{\zeta}, \quad \forall\boldsymbol{c}\in\mathcal{U}_{\rm L}. \tag{51}$$

First, we consider (50) by rewriting it as follows:

$$\left\|\begin{pmatrix}1\\ \boldsymbol{A}\boldsymbol{\zeta}\end{pmatrix}\right\|\leq\tau\sqrt{\frac{P_{\rm S}}{\gamma_{\rm th}^{\rm CE}\sigma_{\rm D}^2}}, \quad \forall\boldsymbol{A}\in\mathcal{U}_{\rm R}. \tag{52}$$

We now replace (52) by[18]

$$\begin{aligned}&0\leq\lambda,\\ &\|\boldsymbol{A}_0\boldsymbol{\zeta}+\breve{\boldsymbol{A}}\boldsymbol{u}\|\leq\lambda, \quad \forall\boldsymbol{u}\in\{\boldsymbol{u}:\|\boldsymbol{u}\|\leq\rho_1\}\end{aligned} \tag{53}$$

where $\lambda=\tau\sqrt{\frac{P_{\rm S}}{\gamma_{\rm th}^{\rm CE}\sigma_{\rm D}^2}}-1$ and we have substituted $\boldsymbol{A}$ defined by the uncertainty set $\mathcal{U}_{\rm R}$ in (46). Now, by expanding (53) in terms of a quadratic form of $\boldsymbol{u}$, we have

$$\begin{aligned}&0\leq\lambda,\\ &0\leq q_0(\boldsymbol{u}), \quad \forall\boldsymbol{u}\in\{\boldsymbol{u}:0\leq q_1(\boldsymbol{u})\}\end{aligned} \tag{54}$$

where

$$\begin{aligned}q_0(\boldsymbol{u}) &= -\boldsymbol{u}^T\breve{\boldsymbol{A}}^T\breve{\boldsymbol{A}}\boldsymbol{u}-2(\breve{\boldsymbol{A}}^T\boldsymbol{A}_0\boldsymbol{\zeta})^T\boldsymbol{u}-\boldsymbol{\zeta}^T\boldsymbol{A}_0^T\boldsymbol{A}_0\boldsymbol{\zeta}+\lambda^2\\ q_1(\boldsymbol{u}) &= \rho_1^2-\boldsymbol{u}^T\boldsymbol{u}.\end{aligned} \tag{55}$$

We exploit the following lemma to express the quadratic constraints in (55) in terms of matrix inequality.

Lemma 1 (S-Procedure [32]): Let $q_0(\boldsymbol{u})=\boldsymbol{u}^T\boldsymbol{B}_0\boldsymbol{u}+2\boldsymbol{b}_0^T\boldsymbol{u}+c_0$ and $q_1(\boldsymbol{u})=\boldsymbol{u}^T\boldsymbol{B}_1\boldsymbol{u}+2\boldsymbol{b}_1^T\boldsymbol{u}+c_1$ be two quadratic functions of $\boldsymbol{u}$, where $\boldsymbol{B}_0$ and $\boldsymbol{B}_1$ are symmetric, and there exists some $\boldsymbol{u}_0$ satisfying $q_1(\boldsymbol{u}_0)>0$. Then, we have

$$q_1(\boldsymbol{u})\geq 0\Rightarrow q_0(\boldsymbol{u})\geq 0 \text{ iff } \exists\alpha\in\mathbb{R}_+ : \begin{bmatrix}\boldsymbol{B}_0 & \boldsymbol{b}_0\\ \boldsymbol{b}_0^T & c_0\end{bmatrix}-\alpha\begin{bmatrix}\boldsymbol{B}_1 & \boldsymbol{b}_1\\ \boldsymbol{b}_1^T & c_1\end{bmatrix}\succeq 0.$$

From Lemma 1, it follows that (54) is satisfied if and only if there exists $\alpha\in\mathbb{R}_+$ such that

$$\begin{bmatrix}-\breve{\boldsymbol{A}}^T\breve{\boldsymbol{A}} & -\breve{\boldsymbol{A}}^T\boldsymbol{A}_0\boldsymbol{\zeta}\\ (-\breve{\boldsymbol{A}}^T\boldsymbol{A}_0\boldsymbol{\zeta})^T & \lambda^2-\boldsymbol{\zeta}^T\boldsymbol{A}_0^T\boldsymbol{A}_0\boldsymbol{\zeta}\end{bmatrix}-\alpha\begin{bmatrix}-\boldsymbol{I}_{N_A} & \boldsymbol{0}_{N_A}\\ \boldsymbol{0}_{N_A}^T & \rho_1^2\end{bmatrix}\succeq 0. \tag{56}$$

[18]It follows from the triangle inequality that if (53) is satisfied, then (52) is always satisfied. Note that with the use of constraint (53), instead of (52), we have converted $\mathcal{RP}_{\rm coh}^{\rm CE}\left(\gamma_{\rm th}^{\rm CE}\right)$ into an SDP.

To convert the above quadratic matrix inequality into a linear matrix inequality (LMI), we first let $\alpha = \lambda\mu$ for some $\mu \in \mathbb{R}_+$. Rearranging (56), we have[19]

$$\Delta_{\boldsymbol{E}} \triangleq \lambda \begin{bmatrix} \mu \boldsymbol{I}_{N_A} & \boldsymbol{0}_{N_A} \\ \boldsymbol{0}_{N_A}^T & \lambda - \mu\rho_1^2 \end{bmatrix} - \begin{bmatrix} \breve{\boldsymbol{A}}^T \\ \boldsymbol{\zeta}^T \boldsymbol{A}_0^T \end{bmatrix} \boldsymbol{I}_K \begin{bmatrix} \breve{\boldsymbol{A}}^T \\ \boldsymbol{\zeta}^T \boldsymbol{A}_0^T \end{bmatrix}^T \succeq 0. \tag{57}$$

To linearize (57), we rely on the following lemma:

Lemma 2 (Schur Complement [32]): Let

$$\boldsymbol{M} = \begin{bmatrix} \boldsymbol{C} & \boldsymbol{D} \\ \boldsymbol{D}^T & \boldsymbol{E} \end{bmatrix}$$

be a symmetric matrix with $\boldsymbol{E} \succ 0$. Then, $\boldsymbol{M} \succeq 0$ if and only if the Schur complement of $\boldsymbol{E}$ in $\boldsymbol{M}$, i.e., $\Delta_{\boldsymbol{E}} = \boldsymbol{C} - \boldsymbol{D}\boldsymbol{E}^{-1}\boldsymbol{D}^T \succeq 0$.

If $\lambda > 0$, it follows that $\frac{1}{\lambda}\Delta_{\boldsymbol{E}}$ in (57) is the Schur complement of $\lambda \boldsymbol{I}_K$ in

$$\boldsymbol{M} \triangleq \begin{bmatrix} \mu \boldsymbol{I}_{N_A} & \boldsymbol{0}_{N_A} & \breve{\boldsymbol{A}}^T \\ \boldsymbol{0}_{N_A}^T & \lambda - \mu\rho_1^2 & \boldsymbol{\zeta}^T \boldsymbol{A}_0^T \\ \breve{\boldsymbol{A}} & \boldsymbol{A}_0\boldsymbol{\zeta} & \lambda \boldsymbol{I}_K \end{bmatrix} \tag{58}$$

and by Lemma 2, $\boldsymbol{M} \succeq 0$ since $\frac{1}{\lambda}\Delta_{\boldsymbol{E}} \succeq 0$. For $\lambda = 0, \boldsymbol{M} \succeq 0$ holds if and only if $\mu = 0, \boldsymbol{A}_0\boldsymbol{\zeta}$ and $\breve{\boldsymbol{A}} = 0$. Thus, we have the first LMI in (49). In summary, a pair $(\boldsymbol{\zeta}, \tau)$ satisfies (50) if there exists some $\mu \in \mathbb{R}_+$ and $\tau \geq \sqrt{\gamma_{\text{th}}^{\text{CE}}\sigma_{\text{D}}^2/P_{\text{S}}}$ such that the triple $(\boldsymbol{\zeta}, \tau, \mu)$ satisfies $\boldsymbol{M} \succeq 0$.

Next, when we turn to (51) and substitute $\boldsymbol{c}$ defined by the uncertainty set $\mathcal{U}_{\text{L}}$ in (47) into (51), we have equivalently

$$\breve{\boldsymbol{c}}^T \boldsymbol{v} \geq -\left(\boldsymbol{c}_0^T\boldsymbol{\zeta} - \tau\right), \quad \forall \boldsymbol{v} \in \{\boldsymbol{v} : \|\boldsymbol{v}\| \leq \rho_2\}. \tag{59}$$

Following similar steps leading to (44), we can express the robust constraint in (59) as

$$\begin{bmatrix} \frac{\boldsymbol{c}_0^T\boldsymbol{\zeta} - \tau}{\rho_2} \\ \breve{\boldsymbol{c}} \end{bmatrix} \succeq_{\mathcal{K}} 0. \tag{60}$$

Using [30], we can represent (60) in the form of an LMI as

$$\begin{bmatrix} \frac{(\boldsymbol{c}_0^T\boldsymbol{\zeta} - \tau)}{\rho_2}\boldsymbol{I}_{N_c} & \breve{\boldsymbol{c}} \\ \breve{\boldsymbol{c}}^T & \frac{(\boldsymbol{c}_0^T\boldsymbol{\zeta} - \tau)}{\rho_2} \end{bmatrix} \succeq 0. \tag{61}$$

Therefore, we obtain the second LMI in (49). The other three LMIs in (49) are easily obtained by representing the SOC constraint in terms of LMIs [30, p. 196]. □

[19] When $\lambda = 0$, we have $\mu = 0$.

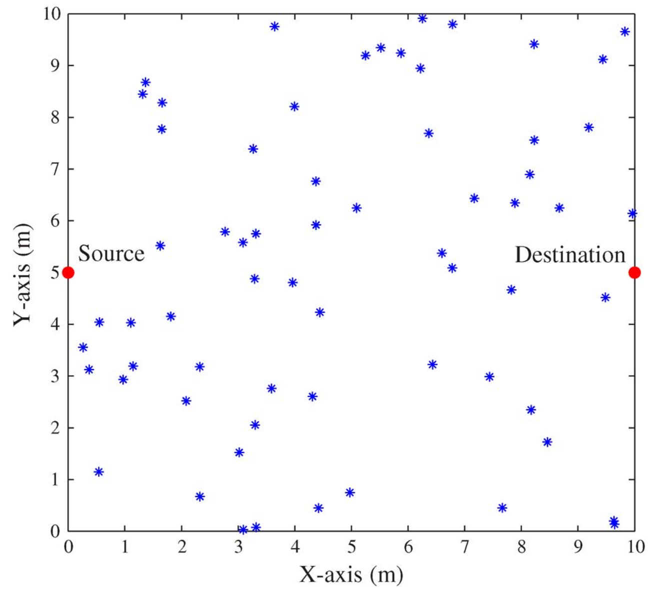

Fig. 1. An example realization of a wireless relay network.

Remark 3: Even if the sidewise independence assumption does not hold, the robust counterpart obtained in Theorem 6 gives us an approximate robust counterpart [36]–[38]. Without any sidewise independence assumption, it is unclear whether a computationally tractable robust counterpart exists [36]–[38]. As a result, the above conservative approach using sidewise independent uncertainty sets becomes attractive.

V. Numerical Results

To illustrate the performance of our proposed algorithms, we consider networks with K relay nodes deployed randomly and independently over a 10 m × 10 m square. For each network, the source and destination nodes are positioned on the opposite sides of the square, i.e., the source node is fixed at $(x, y) = (0 \text{ m}, 5 \text{ m})$ and the destination node is fixed at $(x, y) = (10 \text{ m}, 5 \text{ m})$. One possible realization of the network with $K = 64$ is shown in Fig. 1. For each realization of the random network topology, we generate $S_{\text{B},k}$ and $S_{\text{F},k}$ according to (5) and (6) with $\varepsilon = 4$. This procedure is repeated for 20,000 realizations. The noise variances are normalized such that $\sigma_{\text{R},k}^2 = 1$ and $\sigma_{\text{D}}^2 = 1$. The constraint on the maximum transmission power of each individual relay node is set at $P = 10$ dB. Throughout this section, we use the SeDuMi optimization package [39] to determine the relay power allocations according to our algorithms described in Sections III and IV. The uncertainty sets in Theorems 5 and 6 are chosen such that $N_\Delta = 1, \boldsymbol{\Delta}_1 = \boldsymbol{\Delta}_0, N_A = 1, \boldsymbol{A}_1 = \boldsymbol{A}_0$, and $N_c = 1, \boldsymbol{c}_1 = \boldsymbol{c}_0$. We consider $\rho_0 = \rho_1 = \rho_2 = \rho$, where $\rho = 0$ corresponds to perfect knowledge of the global CSI and $\rho = 1$ corresponds to an uncertainty that is of the same size as the estimated global CSI, i.e., $\boldsymbol{d}_0, \boldsymbol{e}_0, \boldsymbol{A}_0, \boldsymbol{c}_0$.

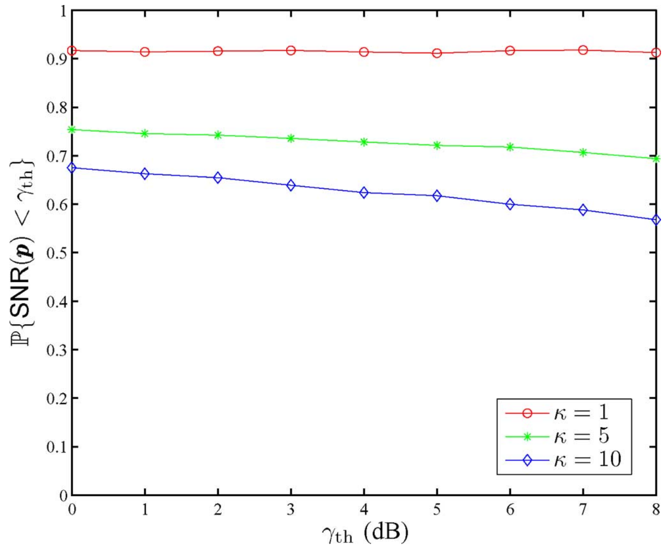

Fig. 2. Outage probability of the noncoherent AF relay network with $K = 64$, $P_{\rm S} = 30$ dB, and $\sigma_{\rm dB} = 8$ dB.

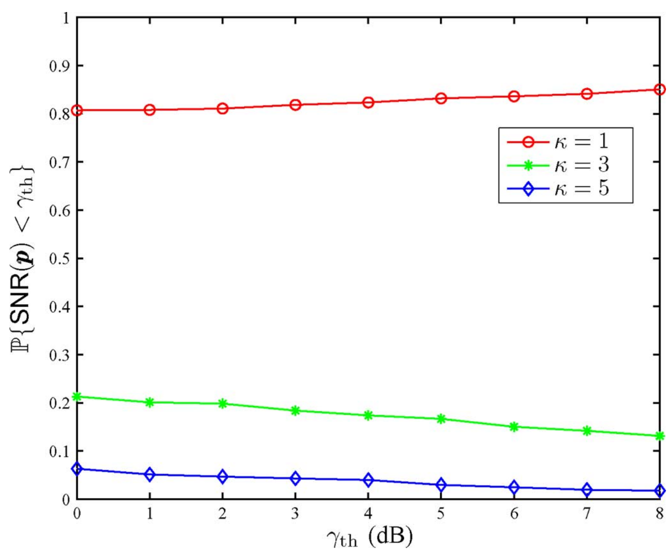

Fig. 3. Outage probability of the coherent AF relay network with $K = 64$, $P_{\rm S} = 30$ dB, and $\sigma_{\rm dB} = 8$ dB.

Figs. 2 and 3 show the outage probabilities (the SNR constraint in (13) is not satisfied) as a function of $\gamma_{\rm th}$ for noncoherent and coherent relay networks, respectively.[20] The power allocations used in these plots were obtained by solving $\mathcal{P}^{\rm CE}_{\rm noncoh}(\gamma^{\rm CE}_{\rm th})$ and $\mathcal{P}^{\rm CE}_{\rm coh}(\gamma^{\rm CE}_{\rm th})$ using our proposed algorithms.[21] It can be seen that the outage probabilities of the noncoherent and coherent AF relay networks decrease as the factor κ increases. This decrease shows that the CE formulation, which enables implementation of practical algorithms that track only large-scale fading, can effectively account for the random fluctuations in the actual instantaneous SNR as well as compensate for the use of approximation in (15). Comparing Figs. 2 and 3, we see that the CE approach is less effective in noncoherent AF relay networks, even

[20]The chosen value of $\sigma_{\rm dB}$ in these plots is typical for macrocellular applications [20].

[21]Recall from Section II-B that the SNR constraint in (13) may not be satisfied even when $\mathcal{P}^{\rm CE}_{\rm noncoh}(\gamma^{\rm CE}_{\rm th})$ and $\mathcal{P}^{\rm CE}_{\rm coh}(\gamma^{\rm CE}_{\rm th})$ are feasible.

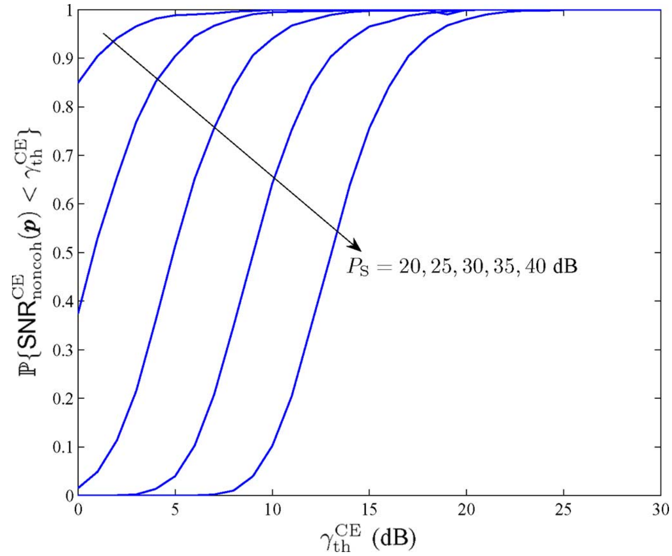

Fig. 4. CE outage probability of the proposed power allocation algorithm for the noncoherent AF relay network as a function of $\gamma^{\rm CE}_{\rm th}$ with $K = 64$ and $\sigma_{\rm dB} = 8$ dB.

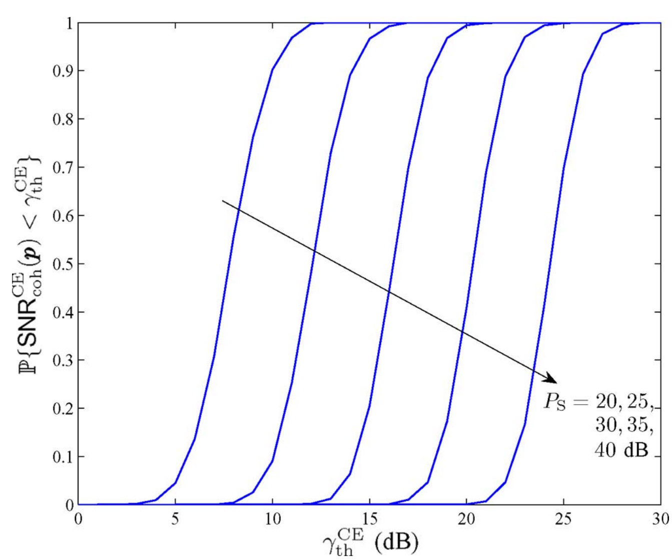

Fig. 5. CE outage probability of the proposed power allocation algorithm for the coherent AF relay network as a function of $\gamma^{\rm CE}_{\rm th}$ with $K = 64$ and $\sigma_{\rm dB} = 8$ dB.

with larger κ values, owing to the absence of phase alignment at the relay nodes.[22]

There may be some situations where $\mathcal{P}^{\rm CE}_{\rm noncoh}(\gamma^{\rm CE}_{\rm th})$ and $\mathcal{P}^{\rm CE}_{\rm coh}(\gamma^{\rm CE}_{\rm th})$ are infeasible. We denote the probabilities of such events as CE outage probabilities, i.e., probabilities that the CE SNR constraints in (18) and (26) are not satisfied. The CE outage probabilities as a function of $\gamma^{\rm CE}_{\rm th}$ are plotted for various values of $P_{\rm S}$ in Figs. 4 and 5 for noncoherent and coherent AF relay networks, respectively. We see from these figures that, for a fixed CE SNR target value, an increase in source power is required to maintain a lower outage probability. This increase in required source power is more drastic in noncoherent AF relay networks compared to coherent AF relay networks.

[22]In such cases, time diversity techniques can be used [28].

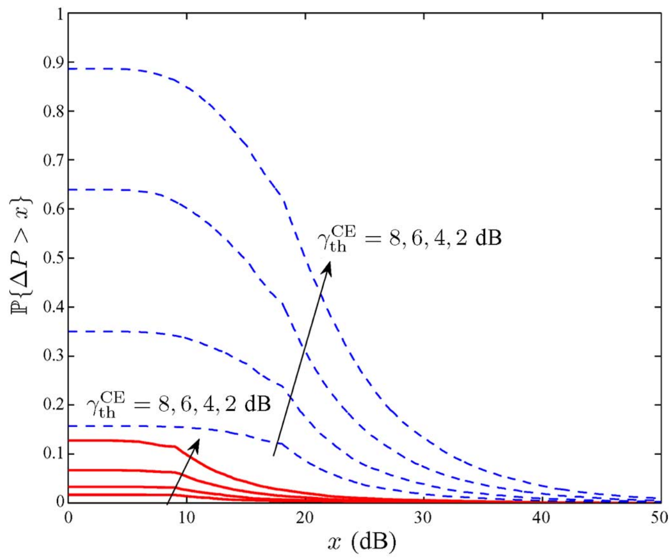

Fig. 6. Ccdf of ΔP of the noncoherent AF relay network for different K and $\gamma_{\rm th}^{\rm CE}$ with $P_{\rm S} = 30$ dB and $\sigma_{\rm dB} = 8$ dB. The solid and dashed lines indicate $K = 8$ and 64, respectively.

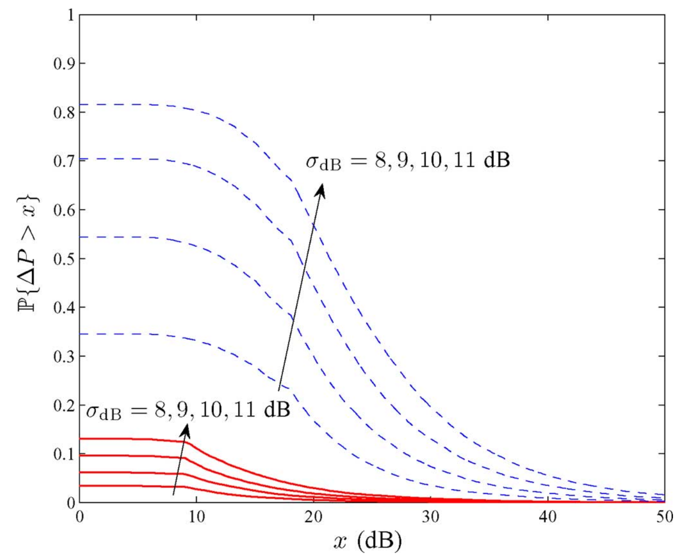

Fig. 8. Ccdf of ΔP of the noncoherent AF relay network for different K and $\sigma_{\rm dB}$ with $P_{\rm S} = 30$ dB and $\gamma_{\rm th}^{\rm CE} = 6$ dB. The solid and dashed lines indicate $K = 8$ and 64, respectively.

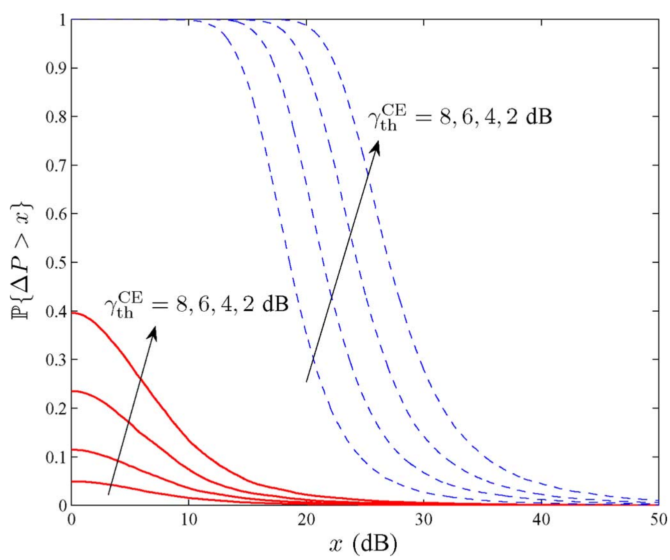

Fig. 7. Ccdf of ΔP of the coherent AF relay network for different K and $\gamma_{\rm th}^{\rm CE}$ with $P_{\rm S} = 30$ dB and $\sigma_{\rm dB} = 8$ dB. The solid and dashed lines indicate $K = 8$ and 64, respectively.

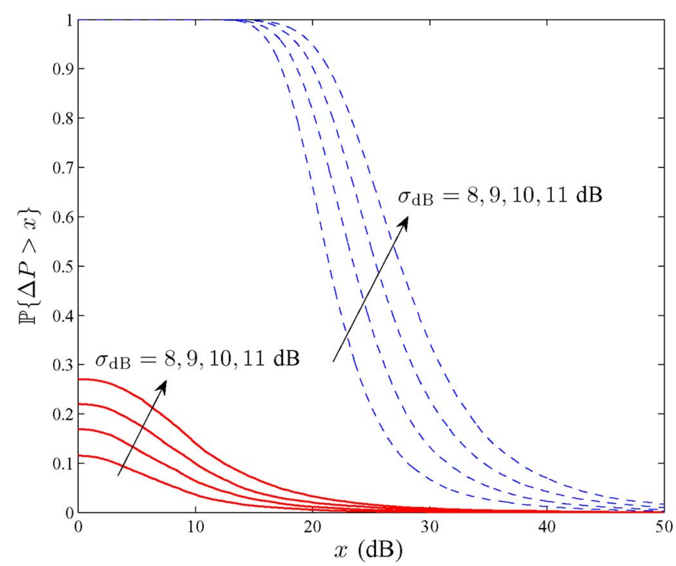

Fig. 9. Ccdf of ΔP of the coherent AF relay network for different K and $\sigma_{\rm dB}$ with $P_{\rm S} = 30$ dB and $\gamma_{\rm th}^{\rm CE} = 6$ dB. The solid and dashed lines indicate $K = 8$ and 64, respectively.

We next compare our power allocation algorithms in terms of power-efficiency ΔP, where $\Delta P \triangleq 10\log(KP/\sum_{k=1}^{K} p_k)$ is defined as the ratio of the total relay transmission power based on the naive scheme and that based on our algorithm.[23] Figs. 6 and 7 show the complementary cumulative distribution function (ccdf) of ΔP for noncoherent and coherent AF relay networks with different numbers of relay nodes and CE SNR target values.[24] We see that our proposed algorithms offer significant power savings in both networks. These figures indicate that ΔP increases when the number of relay nodes increases. This is because our power allocation algorithms exploit the channel variations in the spatial domain. When $\gamma_{\rm th}^{\rm CE}$ decreases, the efficiency increases, since less relay power expenditure is required to satisfy the CE SNR constraint. Comparing Figs. 6 and 7, we see that the increase in power-efficiency is more significant, due to a higher cooperative gain, in coherent AF relay networks compared to noncoherent AF relay networks, as observed in [24].

Figs. 8 and 9 show the ccdf of ΔP for noncoherent and coherent AF relay networks with different numbers of relay nodes and $\sigma_{\rm dB}$. These figures indicate that ΔP increases when $\sigma_{\rm dB}$ increases, implying that our proposed power allocation algorithms are more efficient for channels with large fluctuations. This increase in ΔP is more significant for large networks for the same reason noted in previous paragraph.

[23]Recall that the naive scheme is referred to one that employs maximum transmission power at each relay node.

[24]The ccdf of a r.v. X gives the probability that X is above a particular level.

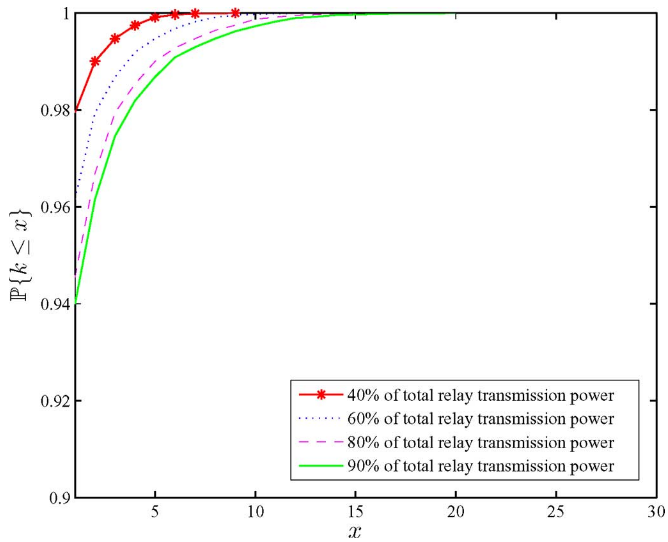

Fig. 10. Effect of relay transmission power on cdf of the number of relay nodes for the noncoherent AF relay network with $K = 64$, $P_{\mathrm{S}} = 30$ dB, $\sigma_{\mathrm{dB}} = 8$ dB, and $\gamma_{\mathrm{th}}^{\mathrm{CE}} = 6$ dB.

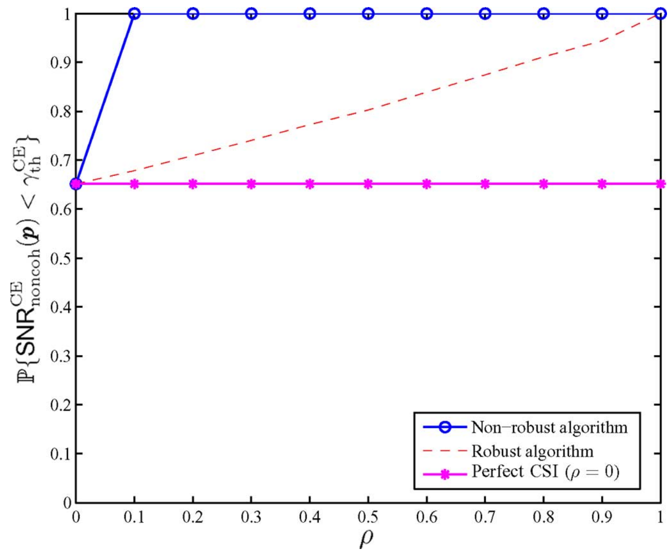

Fig. 12. CE outage probability of robust power allocation algorithms for the noncoherent AF relay network with $K = 64$, $P_{\mathrm{S}} = 30$ dB, $\sigma_{\mathrm{dB}} = 8$ dB, and $\gamma_{\mathrm{th}}^{\mathrm{CE}} = 6$ dB.

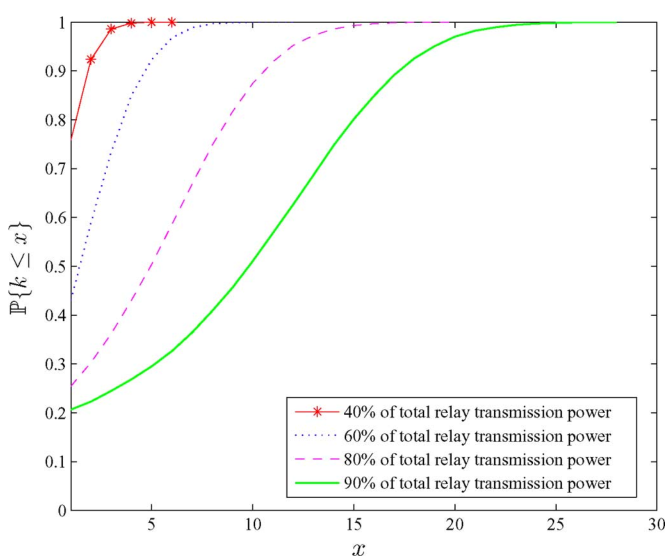

Fig. 11. Effect of relay transmission power on cdf of the number of relay nodes for the coherent AF relay network with $K = 64$, $P_{\mathrm{S}} = 30$ dB, $\sigma_{\mathrm{dB}} = 8$ dB, and $\gamma_{\mathrm{th}}^{\mathrm{CE}} = 6$ dB.

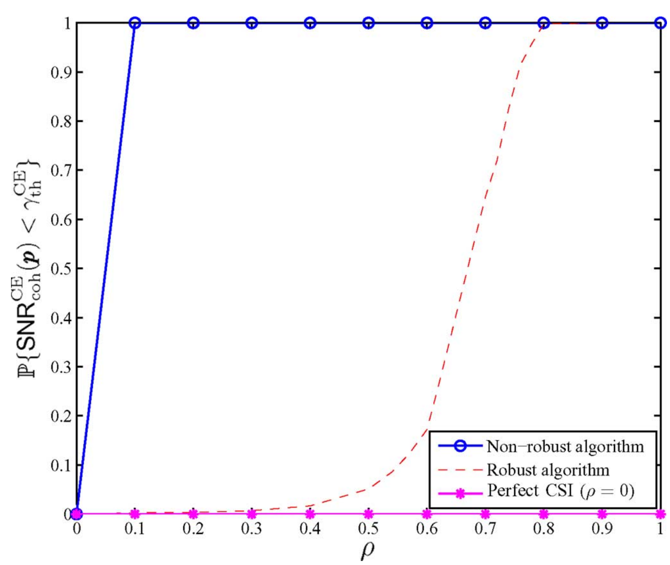

Fig. 13. CE outage probability of robust power allocation algorithms for the coherent AF relay network with $K = 64$, $P_{\mathrm{S}} = 30$ dB, $\sigma_{\mathrm{dB}} = 8$ dB, and $\gamma_{\mathrm{th}}^{\mathrm{CE}} = 6$ dB.

Figs. 10 and 11 show the cumulative distribution function (cdf) of the minimum number of relay nodes that are necessary to achieve a certain percentage of the total relay transmission power in noncoherent and coherent AF relay networks, respectively. We observe that most of the total relay transmission power tends to be distributed among a smaller subset of relay nodes in the noncoherent case, compared to the coherent case. This suggests that relay selection is beneficial in noncoherent AF relay networks as observed in [7].

Lastly, we compare the robust algorithms in terms of the CE outage probabilities. Figs. 12 and 13 show the CE outage probability as a function of the size of the uncertainty set ρ for noncoherent and coherent AF relay networks, respectively. We observe from these figures that adopting non-robust algorithms, i.e., simply ignoring uncertainties in the global CSI, results in a high penalty in terms of outage probability. On the other hand, we clearly see that robust algorithms provide lower outage probabilities compared to non-robust algorithms.

VI. Conclusion

In this paper, we formulated the AF relay power allocation problem as the total relay transmission power minimization problem subject to a QoS constraint. Under the CE output SNR constraint, we proposed practical algorithms that track only large-scale fading. Under perfect knowledge of the large-scale fading, we showed that the optimization problems for the noncoherent and coherent AF relay networks can be cast as an LP and an SOCP, respectively. The conditions for verifying the feasibility of these problems and the optimality of the solutions are also derived. Furthermore, we extended these optimization problems to take into account uncertainties in the knowledge of large-scale fading. For ellipsoidal uncertainty sets, we showed that the robust counterparts of our optimization problems for the noncoherent and coherent AF relay networks can be formulated as an SOCP and an SDP, respectively. Numerical results showed that the proposed algorithms provide significant power savings over the naive scheme that employs maximum transmission power at each relay node. In addition, our robust algorithms provide effective and feasible solutions, yielding good performance in the presence of uncertainties associated with the global CSI. In summary, this work highlights the importance of practical and robust algorithms in realistic wireless networks.

Appendix I
Proof of Theorem 2

First, we set up the Lagrangian function $L : \mathbb{R}^K \times \mathbb{R}^{2K+1}$ associated with the primal problem (19) as

$$L(\boldsymbol{p}, \boldsymbol{\nu}) = -\boldsymbol{m}^T\boldsymbol{\nu} + (\boldsymbol{B}^T\boldsymbol{\nu} + \mathbf{1})^T\boldsymbol{p} \tag{62}$$

where $\boldsymbol{\nu}$ is the Lagrange multipliers corresponding to the linear constraints in (19). The dual problem $\mathcal{DP}_{\rm noncoh}^{\rm CE}(\gamma_{\rm th}^{\rm CE})$ is given by

$$\begin{aligned} &\max_{\boldsymbol{\nu}} \ -\boldsymbol{m}^T\boldsymbol{\nu} \\ &\text{s.t.} \quad \boldsymbol{B}^T\boldsymbol{\nu} + \mathbf{1} = \mathbf{0} \\ &\qquad\qquad \boldsymbol{\nu} \succeq \mathbf{0}. \end{aligned} \tag{63}$$

For LP, strong duality holds when either one of the primal or dual problems is feasible [29], [32]. Thus, $(\boldsymbol{p}_{\rm opt}, \boldsymbol{\nu}_{\rm opt})$ are optimal if and only if they satisfy the following three conditions.

Feasibility condition of the primal problem:

$$\boldsymbol{B}\boldsymbol{p}_{\rm opt} \le \boldsymbol{m},$$

Feasibility conditions of the dual problem:

$$\begin{aligned} &\boldsymbol{B}^T\boldsymbol{\nu}_{\rm opt} + \mathbf{1} = \mathbf{0}, \\ &\nu_{k,{\rm opt}} \ge 0, \quad k = 1, \ldots, K, \end{aligned}$$

Zero duality gap condition:

$$\mathbf{1}^T\boldsymbol{p}_{\rm opt} + \boldsymbol{m}^T\boldsymbol{\nu}_{\rm opt} = 0.$$

Appendix II
Proof of Proposition 1

The necessary and sufficient condition for $\mathcal{P}_{\rm coh}^{\rm CE}(\gamma_{\rm th}^{\rm CE})$ to be feasible can be immediately obtained by maximizing the right-hand side of the CE SNR constraint in (26) with respect to all possible $\boldsymbol{\zeta}$. This maximization can be formulated as an optimization problem in (33), which is shown to be quasiconvex [24] with a non-empty feasible set since $P > 0$. To derive (34), we first note that

$$\frac{\gamma_{\rm th}^{\rm CE}\sigma_{\rm D}^2}{P_{\rm S}} < \max_{\boldsymbol{\zeta}\in\mathcal{X}_\zeta} \left(\frac{(\boldsymbol{c}^T\boldsymbol{\zeta})^2}{\|\boldsymbol{A}\boldsymbol{\zeta}\|^2} \right) \tag{64}$$

since the right-hand side of (64) is strictly greater than the right-hand side of (32). The right-hand side of (64) can be further bounded by

$$\max_{\boldsymbol{\zeta}\in\mathcal{X}_\zeta} \left(\frac{(\boldsymbol{c}^T\boldsymbol{\zeta})^2}{\|\boldsymbol{A}\boldsymbol{\zeta}\|^2} \right) \le \frac{\|\boldsymbol{c}\|^2}{\min_{\boldsymbol{\zeta}\in\mathcal{X}_\zeta} \frac{\|\boldsymbol{A}\boldsymbol{\zeta}\|^2}{\|\boldsymbol{\zeta}\|^2}} \tag{65}$$

where we have applied the Cauchy–Schwartz inequality to the vectors $\boldsymbol{c}$ and $\boldsymbol{\zeta}$. From (65), we apply the Rayleigh-Ritz theorem to obtain the desired result [40, p. 176].

Appendix III
Proof of Theorem 4

First, we set up the Lagrangian function $L : \mathbb{R}^K \times \mathbb{R} \times \mathbb{R}^K \times \mathbb{R}^K$ associated with the primal problem (26) as

$$L(\boldsymbol{\zeta}, \mu, \boldsymbol{\lambda}, \boldsymbol{\nu}) = \frac{\mu\gamma_{\rm th}^{\rm CE}\sigma_{\rm D}^2}{P_{\rm S}} - {\rm tr}(\boldsymbol{\Lambda}) + \boldsymbol{\zeta}^T(\boldsymbol{I}_K + \mu\boldsymbol{Q})\boldsymbol{\zeta} + \boldsymbol{\zeta}^T(\boldsymbol{\lambda} - \boldsymbol{\nu}) \tag{66}$$

where μ, $\boldsymbol{\lambda}$, and $\boldsymbol{\nu}$ are the Lagrange multipliers corresponding to the CE SNR constraint and power constraints in (26), respectively. The dual problem $\mathcal{DP}_{\rm coh}^{\rm CE}(\gamma_{\rm th}^{\rm CE})$ is given by

$$\begin{aligned} &\max_{\mu,\boldsymbol{\lambda},\boldsymbol{\nu}} \ g(\mu, \boldsymbol{\lambda}, \boldsymbol{\nu}) \\ &\text{s.t.} \qquad \boldsymbol{I}_K + \mu\boldsymbol{Q} \succ 0 \end{aligned} \tag{67}$$

where the dual feasible variables are $\mu \in \mathbb{R}_+$, $\boldsymbol{\lambda} \in \mathbb{R}_+^K$, and $\boldsymbol{\nu} \in \mathbb{R}_+^K$. Under some constraint qualifications, strong duality holds.[25] In this case, the KKT optimality conditions are both necessary and sufficient, and the optimal solutions of the primal and dual problems, $\boldsymbol{\zeta}_{\rm opt} \in \mathbb{R}_+^K$ and $(\mu_{\rm opt}, \boldsymbol{\lambda}_{\rm opt}, \boldsymbol{\nu}_{\rm opt}) \in \mathbb{R}_+ \times \mathbb{R}_+^K \times \mathbb{R}_+^K$, must satisfy the following three conditions.

Feasibility conditions:

$$\begin{aligned} &\frac{\gamma_{\rm th}^{\rm CE}\sigma_{\rm D}^2}{P_{\rm S}} + \boldsymbol{\zeta}_{\rm opt}^T\boldsymbol{Q}\boldsymbol{\zeta}_{\rm opt} \le 0, \\ &\zeta_{k,{\rm opt}} - \sqrt{P} \le 0, \quad k = 1, \ldots, K \\ &-\zeta_{k,{\rm opt}} \le 0, \quad k = 1, \ldots, K, \end{aligned}$$

Complementary slackness conditions:

$$\begin{aligned} &\mu_{\rm opt}\left(\frac{\gamma_{\rm th}^{\rm CE}\sigma_{\rm D}^2}{P_{\rm S}} + \boldsymbol{\zeta}_{\rm opt}^T\boldsymbol{Q}\boldsymbol{\zeta}_{\rm opt} \right) = 0, \\ &\lambda_{k,{\rm opt}}(\zeta_{k,{\rm opt}} - \sqrt{P}) = 0, \quad k = 1, \ldots, K \\ &-\nu_{k,{\rm opt}}\zeta_{k,{\rm opt}} = 0, \quad k = 1, \ldots, K, \end{aligned}$$

[25] One simple version of the constraint qualifications is Slater's condition [32].

Stationarity condition:

$$\nabla_{\boldsymbol{\zeta}} L(\boldsymbol{\zeta}_{\mathrm{opt}}, \mu_{\mathrm{opt}}, \boldsymbol{\lambda}_{\mathrm{opt}}, \boldsymbol{\nu}_{\mathrm{opt}}) = 0.$$

Using (66), we can evaluate the stationarity condition to obtain

$$\boldsymbol{\zeta}_{\mathrm{opt}} = -\frac{1}{2}(\boldsymbol{I}_K + \mu_{\mathrm{opt}}\boldsymbol{Q})^{-1}(\boldsymbol{\lambda}_{\mathrm{opt}} - \boldsymbol{\nu}_{\mathrm{opt}}) \qquad (68)$$

where (68) has a unique $\boldsymbol{\zeta}_{\mathrm{opt}}$ since the matrix $(\boldsymbol{I}_K + \mu_{\mathrm{opt}}\boldsymbol{Q})$ is positive definite. Furthermore, using the complementary slackness condition, we have $\mu_{\mathrm{opt}} > 0$ since $\boldsymbol{\zeta}_{\mathrm{opt}}$ must satisfy the CE SNR constraint with equality when the primal problem is feasible [41]. Combining the above results, we obtain

$$\mu_{\mathrm{opt}} > -\frac{1}{\tau_{\min}(\boldsymbol{Q})} \qquad (69)$$

where we have used the fact that the eigenvalues of a positive definite matrix are strictly positive and $\tau_{\min}(\boldsymbol{I}_K + \mu\boldsymbol{Q}) = 1 + \mu\tau_{\min}(\boldsymbol{Q})$.

ACKNOWLEDGMENT

The authors gratefully acknowledge helpful discussions with M. Chiani and D. Dardari. They would also like to thank the Associate Editor and the anonymous reviewers for their suggestions and careful reading of the manuscript.

REFERENCES

[1] S. Cui, J. Xiao, A. Goldsmith, Z.-Q. Luo, and H. V. Poor, "Estimation diversity and energy efficiency in distributed sensing," *IEEE Trans. Signal Process.*, vol. 55, no. 9, pp. 4683–4695, Sep. 2007.

[2] Y.-W. Hong, W.-J. Huang, F.-H. Chiu, and C.-C. J. Kuo, "Cooperative communications in resource-constrained wireless networks," *IEEE Signal Process. Mag.*, vol. 24, no. 3, pp. 47–57, May 2007.

[3] R. Pabst *et al.*, "Relay-based deployment concepts for wireless and mobile broadband radio," *IEEE Commun. Mag.*, vol. 42, no. 9, pp. 80–89, Sep. 2004.

[4] J. N. Laneman, D. N. C. Tse, and G. W. Wornell, "Cooperative diversity in wireless networks: Efficient protocols and outage behavior," *IEEE Trans. Inform. Theory*, vol. 50, no. 12, pp. 3062–3080, Dec. 2004.

[5] V. Stanković, A. Høst-Madsen, and Z. Xiong, "Cooperative diversity for wireless ad hoc networks," *IEEE Signal Process. Mag.*, vol. 23, no. 5, pp. 37–49, Sep. 2006.

[6] A. Bletsas, H. Shin, and M. Z. Win, "Outage optimality of opportunistic amplify-and-forward relaying," *IEEE Commun. Lett.*, vol. 11, no. 3, pp. 261–263, Mar. 2007.

[7] A. Bletsas, H. Shin, and M. Z. Win, "Cooperative communications with outage-optimal opportunistic relaying," *IEEE Trans. Wireless Commun.*, vol. 6, no. 9, pp. 3450–3460, Sep. 2007.

[8] J. Luo, R. S. Blum, L. Cimini, L. Greenstein, and A. Haimovich, "Decode-and-forward cooperative diversity with power allocation in wireless networks," *IEEE Trans. Wireless Commun.*, vol. 6, no. 3, pp. 793–799, Mar. 2007.

[9] R. Madan, N. Mehta, A. F. Molisch, and J. Zhang, "Energy-efficient cooperative relaying over fading channels with simple relay selection," in *Proc. IEEE Global Telecomm. Conf.*, San Francisco, CA, Nov. 2006, pp. 1–6.

[10] I. Maric and R. D. Yates, "Forwarding strategies for Gaussian parallel-relay networks," in *Proc. Conf. on Inform. Sci. and Sys.*, Princeton, NJ, Mar. 2004.

[11] M. Dohler, A. Gkelias, and H. Aghvami, "Resource allocation for FDMA-based regenerative multihop links," *IEEE Trans. Wireless Commun.*, vol. 3, no. 6, pp. 1989–1993, Nov. 2004.

[12] M. Chen, S. Serbetli, and A. Yener, "Distributed power allocation for parallel relay networks," in *Proc. IEEE Global Telecomm. Conf.*, St. Louis, MO, Nov. 2005, vol. 3, pp. 1177–1181.

[13] T. C.-Y. Ng and W. Yu, "Joint optimization of relay strategies and resource allocations in cooperative cellular networks," *IEEE J. Select. Areas Commun.*, vol. 25, no. 2, pp. 328–339, Feb. 2007.

[14] A. Høst-Madsen and J. Zhang, "Capacity bounds and power allocation for wireless relay channels," *IEEE Trans. Inform. Theory*, vol. 51, no. 6, pp. 2020–2040, Jun. 2005.

[15] D. Brown, "Resource allocation for cooperative transmission in wireless networks," in *Proc. Asilomar Conf. on Signals, Systems and Computers*, Pacific Grove, CA, Nov. 2004, vol. 2, pp. 1473–1477.

[16] K. G. Seddik, A. K. Sadek, W. Su, and K. J. R. Liu, "Outage analysis and optimal power allocation for multi-node amplify-and-forward relay networks," *IEEE Signal Process. Lett.*, vol. 14, no. 6, pp. 377–380, Jun. 2007.

[17] I. Maric and R. D. Yates, "Bandwidth and power allocation for cooperative strategies in Gaussian relay networks," in *Proc. Asilomar Conf. on Signals, Systems and Computers*, Pacific Grove, CA, Nov. 2004, vol. 2, pp. 1907–1911.

[18] A. Conti, M. Z. Win, and M. Chiani, "Slow adaptive M-QAM with diversity in fast fading and shadowing," *IEEE Trans. Commun.*, vol. 55, no. 5, pp. 895–905, May 2007.

[19] A. F. Molisch, *Wireless Communications*, 1st ed. Piscataway, NJ: IEEE Press/Wiley, 2005, 08855-1331.

[20] A. Goldsmith, *Wireless Communications*. Cambridge, U.K.: Cambridge Univ. Press, 2006.

[21] M. O. Hasna and M.-S. Alouini, "A performance study of dual-hop transmissions with fixed gain relays," *IEEE Trans. Wireless Commun.*, vol. 3, no. 6, pp. 1963–1968, Nov. 2004.

[22] R. U. Nabar, H. Bölcskei, and F. W. Kneubühler, "Fading relay channels: Performance limits and space-time signal design," *IEEE J. Sel. Areas Commun.*, vol. 22, no. 6, pp. 1099–1109, Aug. 2004.

[23] M. Gastpar and M. Vetterli, "On the capacity of large Gaussian relay networks," *IEEE Trans. Inform. Theory*, vol. 51, no. 3, pp. 765–779, Mar. 2005.

[24] T. Q. S. Quek, H. Shin, M. Z. Win, and M. Chiani, "Optimal power allocation for amplify-and-forward relay networks via conic programming," in *Proc. IEEE Int. Conf. Commun.*, Glasgow, U.K., June 2007, pp. 5058–5063.

[25] S. Kandukuri and S. Boyd, "Optimal power control in interference-limited fading wireless channels with outage-probability specifications," *IEEE Trans. Wireless Commun.*, vol. 1, no. 1, pp. 46–55, Jan. 2002.

[26] J. Papandriopoulos, J. Evans, and S. Dey, "Optimal power control for Rayleigh-faded multiuser systems with outage constraints," *IEEE Trans. Wireless Commun.*, vol. 4, no. 6, pp. 2705–2715, Nov. 2005.

[27] M. Andersin and Z. Rosberg, "Time variant power control in cellular networks," in *Proc. IEEE Int. Symp. on Personal, Indoor and Mobile Radio Commun.*, Taipei, Taiwan, Oct. 1996, vol. 1, pp. 193–197.

[28] S. V. Hanly, "Capacity and power control in spread spectrum macrodiversity radio networks," *IEEE Trans. Commun.*, vol. 44, no. 2, pp. 247–256, Feb. 1996.

[29] D. Bertsimas and J. N. Tsitsiklis, *Introduction to Linear Optimization*, 1st ed. Belmont, MA: Athena Scientific, 1997, 02178-9998.

[30] M. S. Lobo, L. Vandenberghe, S. Boyd, and H. Lebret, "Applications of second-order cone programming," *Linear Algebra Applicat.*, vol. 284, pp. 193–228, Nov. 1998.

[31] D. P. Bertsekas, A. Nedic, and A. E. Ozdaglar, *Convex Analysis and Optimization*. Belmont, MA: Athena Scientific, 2003.

[32] S. Boyd and L. Vandenberghe, *Convex Optimization*. Cambridge, UK: Cambridge Univ. Press, 2004.

[33] A. Ben-Tal and A. Nemirovski, "Robust convex optimization," *Math. Oper. Res.*, vol. 21, no. 4, pp. 769–805, Nov. 1998.

[34] L. E. Ghaoui, F. Oustry, and H. Lebret, "Robust solutions to uncertain semidefinite programs," *SIAM J. Optim.*, vol. 9, no. 1, pp. 33–52, 1998.

[35] A. Pascual-Iserte, D. P. Palomar, A. I. Pérez-Neira, and M. Á. Lagunas, "A robust maximin approach for MIMO communiations with imperfect channel state information based on convex optimization," *IEEE Trans. Signal Process.*, vol. 54, no. 1, pp. 346–360, Jan. 2006.

[36] A. Ben-Tal and A. Nemirovski, "Robust optimization—Methodology and applications," *Math. Program. Ser. B*, vol. 92, no. 3, pp. 453–480, 2002.

[37] A. Ben-Tal, A. Nemirovski, and C. Roos, "Robust solutions of uncertain quadratic and conic-quadratic problems," *SIAM J. Optim.*, vol. 13, no. 2, pp. 535–560, 2002.

[38] D. Bertsimas and M. Sim, "Tractable approximations to robust conic optimization problems," *Math. Program. Ser B*, vol. 107, pp. 5–36, 2006.

[39] J. Sturm, "Using SeDuMi 1.02, a MATLAB toolbox for optimization over symmetric cones," *Optim. Meth. Softw.*, vol. 11–12, pp. 625–653, Aug. 1999.

[40] R. A. Horn and C. R. Johnson, *Matrix Analysis*, 1st ed. Cambridge: Cambridge Univ. Press, 1990.

[41] J. Zander, "Performance of optimum transmitter power control in cellular radio systems," *IEEE Trans. Veh. Technol.*, vol. 41, no. 1, pp. 57–62, Feb. 1992.

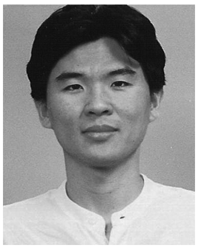

Tony Q. S. Quek (S'98) received the B.E. and M.E. degrees in electrical and electronics engineering from Tokyo Institute of Technology, Tokyo, Japan, in 1998 and 2000, respectively.

From 2001 to 2002, he was with Centre for Wireless Communications, Singapore, as a Research Engineer. Since 2002, he has been with the Laboratory for Information and Decision Systems (LIDS), Massachusetts Institute of Technology (MIT), Cambridge, where he is now pursuing the Ph.D. degree. His research interests include wireless communications, information theory, and optimization theory with special emphasis on ultrawide bandwidth systems, and design of robust and efficient wireless networks.

Mr. Quek received the Singapore Government Scholarship in 1993, Tokyu Foundation Fellowship in 1998, and the ASTAR National Science Scholarship in 2002. He served as member of the Technical Program Committee (TPC) for the IEEE International Conference on Communications (ICC) in 2008, the IEEE Vehicular Technology Conference Spring 2008, IEEE International Symposium on Personal, Indoor and Mobile Radio Communications 2008, the IEEE ICC in 2007, the IEEE Conference on Ultra Wideband in 2006, and the IEEE ICC in 2004.

Hyundong Shin (S'01–M'04) received the B.S. degree in electronics engineering from Kyung Hee University, Korea, in 1999, and the M.S. and Ph.D. degrees in electrical engineering from Seoul National University, Seoul, Korea, in 2001 and 2004, respectively.

From September 2004 to February 2006, he was a Postdoctoral Associate at the Laboratory for Information and Decision Systems (LIDS), Massachusetts Institute of Technology (MIT), Cambridge. In March 2006, he joined the faculty of the School of Electronics and Information, Kyung Hee University, Korea, where he is now an Assistant Professor at the Department of Radio Communication Engineering. His research interests include wireless communications, information and coding theory, cooperative/collaborative communications, and multiple-antenna wireless communication systems and networks.

Dr. Shin served on the Technical Program Committees for the 2006 IEEE International Conference on Communications (ICC'06) and the 2006 IEEE International Conference on Ultra Wideband (ICUWB'06). He currently serves as an Editor for IEEE TRANSACTIONS ON WIRELESS COMMUNICATIONS. He is a Guest Editor for the 2007 *EURASIP Journal on Advances in Signal Processing* (Special Issue on Wireless Cooperative Networks).

Moe Z. Win (S'85-M'87-SM'97-F'04) received the B.S. degree (magna cum laude) from Texas A&M University, College Station, in 1987 and the M.S. degree from the University of Southern California (USC), Los Angeles, in 1989, both in electrical engineering. As a Presidential Fellow at USC, he received both an M.S. degree in applied mathematics and the Ph.D. degree in electrical engineering in 1998.

He is an Associate Professor at the Laboratory for Information & Decision Systems (LIDS), Massachusetts Institute of Technology (MIT), Cambridge. Prior to joining MIT, he spent five years at AT&T Research Laboratories and seven years at the Jet Propulsion Laboratory. His main research interests are the applications of mathematical and statistical theories to communication, detection, and estimation problems. Specific current research topics include measurement and modeling of time-varying channels, design and analysis of multiple antenna systems, ultra-wide bandwidth (UWB) systems, optical transmission systems, and space communications systems.

Dr. Win has been actively involved in organizing and chairing a number of international conferences. He served as the Technical Program Chair for the IEEE Conference on Ultra Wideband in 2006, the IEEE Communication Theory Symposia of ICC-2004 and Globecom-2000, and the IEEE Conference on Ultra Wideband Systems and Technologies in 2002; Technical Program Vice-Chair for the IEEE International Conference on Communications in 2002; and the Tutorial Chair for the IEEE Semiannual International Vehicular Technology Conference in Fall 2001. He served as the chair (2004–2006) and secretary (2002–2004) for the Radio Communications Committee of the IEEE Communications Society. He is currently an Editor for IEEE TRANSACTIONS ON WIRELESS COMMUNICATIONS. He served as Area Editor for Modulation and Signal Design (2003–2006), Editor for Wideband Wireless and Diversity (2003–2006), and Editor for Equalization and Diversity (1998–2003), all for the IEEE TRANSACTIONS ON COMMUNICATIONS. He was Guest-Editor for the 2002 IEEE JOURNAL ON SELECTED AREAS IN COMMUNICATIONS (Special Issue on Ultra-Wideband Radio in Multiaccess Wireless Communications). He received the International Telecommunications Innovation Award from Korea Electronics Technology Institute in 2002, a Young Investigator Award from the Office of Naval Research in 2003, and the IEEE Antennas and Propagation Society Sergei A. Schelkunoff Transactions Prize Paper Award in 2003. In 2004, he was named Young Aerospace Engineer of the Year by AIAA, and garnered the Fulbright Foundation Senior Scholar Lecturing and Research Fellowship, the Institute of Advanced Study Natural Sciences and Technology Fellowship, the Outstanding International Collaboration Award from the Industrial Technology Research Institute of Taiwan, and the Presidential Early Career Award for Scientists and Engineers from the United States White House. He was honored with the 2006 IEEE Eric E. Sumner Award "for pioneering contributions to ultra-wide band communications science and technology." He is an IEEE Distinguished Lecturer and elected Fellow of the IEEE, cited "for contributions to wideband wireless transmission."